Epithelial-Mesenchymal Wnt Crosstalk Directs Planar Cell Polarity in the Developing Cochlea

Ippei Kishimoto[1], Abel P. David[2, 3], Kevin P. Rose[4], Balasubramanian Narasimhan[5], Bradley Efron[5], Sara E. Billings[1], Erin L. Su[1], Wuxing Dong[1], Taha A. Jan[6], Ronna Hertzano[4], Alan G. Cheng[1, *]

[1]Department of Otolaryngology-Head and Neck Surgery, Stanford University School of Medicine, Stanford, CA 94305, USA
[2]Department of Otolaryngology-Head & Neck Surgery, Northwestern Medicine, Chicago, IL 60611, USA
[3]Feinberg School of Medicine, Northwestern University, Chicago, IL 60611, USA
[4]Section on Omics and Translational Science of Hearing, Neurotology Branch, National Institute on Deafness and Other Communication Disorders, National Institutes of Health, Bethesda, MD 20892, USA
[5]Department of Statistics, Stanford University, Stanford, CA 94305, USA
[6]Department of Otolaryngology - Head and Neck Surgery, Epithelial Biology Center, Vanderbilt Center for Stem Cell Biology, Vanderbilt University Medical Center, Nashville, TN 37232, USA

Short title: Epithelial and mesenchymal Wnts regulate cochlear development

Abstract: 180 words
Text: 7,657 words
Figures: 6
Supplemental items: 11 figures, 1 table, 1 source data

*Corresponding author
Alan G. Cheng, M.D.
801 Welch Road
Department of Otolaryngology-HNS
Stanford, CA 94305
Phone: (650) 725-6500
Fax: (650) 721-2163
Email: aglcheng@stanford.edu

Abstract:

Cochlear hair cells are crucial for sound transduction and are precisely oriented by planar cell polarity (PCP). Wnt proteins direct PCP in vertebrates, but their roles in regulating cochlear PCP remain unclear. Here, we inhibited Wnt secretion by ablating Wntless in the cochlear epithelium and found shortened cochlea, mild hair cell misorientation and mislocalization of PCP proteins, Fzd6 and Dvl2, representing defects less severe than classic PCP mutants. Computational cell-communication analysis predicted that candidate Wnts from the cochlear epithelium (Wnt5a, Wnt7a, Wnt7b) and surrounding periotic mesenchyme (Wnt5a) act on developing hair cells. Deletion of Wnt5a, Wnt7a, and Wnt7b additively shortened the cochlea without causing hair cell misorientation or mislocalization of PCP proteins. Moreover, deletion of Wnt5a alone in the periotic mesenchyme failed to cause PCP defects. However, ablating both epithelial and mesenchymal Wnts caused a severely shortened cochlea with apically malrotated hair cells devoid of polarized core PCP proteins. Thus, Wnts serve as global instructive cues directing cochlear outgrowth and hair cell polarization, with remarkable redundancy of distinct Wnts across epithelial and mesenchymal compartments to ensure a fail-safe developmental program.

Key words: cochlea, development, hair cells, Wnt, planar cell polarity

65 **Introduction**

66 The cochlea is a spiral-shaped sensory organ critical for sound transduction. As
67 mechanotransducers of sound vibration, hair cells are precisely arranged both
68 tonotopically along the length of the cochlea and radially to form three rows of outer hair
69 cells (OHCs) and one row of inner hair cells (IHCs).

70 During embryonic development in mice, the cochlear duct initially forms as an
71 outpouching from the ventral otocyst at embryonic day (E) 11 and subsequently elongates
72 to become a two-and-a-half-turn organ[1, 2]. In the floor of the cochlear duct, terminal
73 mitosis of prosensory cells begins in the apex and extends towards the base, with hair
74 cell specification occurring in the opposite direction between E12.5 and E14.5[2, 3, 4]. Four
75 rows of hair cells and interdigitating supporting cells are arranged in a checkerboard
76 pattern and a precise radial orientation, ensuring that hair bundles, which house the
77 mechanotransduction machinery, uniformly face laterally. This organized cochlear
78 patterning is regulated by the planar cell polarity (PCP) pathway.

79 The PCP pathway is evolutionarily conserved from Drosophila to mammals,
80 governing both convergent extension and hair cell polarity in the developing mouse
81 cochlea[5, 6]. In humans, mutations underlying Bardet–Biedl syndrome[7] and Alstrom
82 syndrome[8, 9] disrupt PCP signaling and cochlear hair cell development, resulting in
83 hearing loss. In mammals, there are six groups of core PCP proteins-Frizzled (Fzd), Van
84 Gogh (Vangl), Celsr1, Dishevelled (Dvl), Prickle (Pk), and Diego (Dgo)-all of which are
85 asymmetrically expressed at opposite poles of cochlear hair cells and supporting cells[10,
86 11, 12, 13, 14, 15]. Deletion of Celsr1 or Vangl2 causes cochlear shortening and severe
87 misorientation of hair cells[16, 17], whereas mutants of Vangl1 displayed relatively mild PCP

88 defects[16]. Concurrent deletion of Fzd3/Fzd6 or Dvl1/Dvl2 leads to striking PCP defects[12,
89 14], and deletion of other core PCP proteins in the presence of the Vangl2 looptail mutation
90 amplifies the severity[16], suggesting complementary and redundant roles among core PCP
91 proteins.

92 Wnt signaling plays multiple essential roles during development, including cell
93 differentiation, proliferation, cell polarity, and tissue patterning[18, 19]. The Wnt signaling
94 pathway can be broadly classified as canonical and non-canonical, where the former is
95 mediated by β-catenin and the latter by PCP signaling[20]. In the cochlea, Wnt/β-catenin
96 signaling is required for hair cell specification[21], radial patterning[22], and supporting cell
97 specification[23]. In vertebrates, although Wnts are known to regulate PCP signaling in
98 various organs such as the neural tube, muscles, and limbs[24, 25], whether this occurs in
99 the cochlea is unclear.

100 Among the 19 Wnt ligands in mammals, Wnt2b, Wnt4, Wnt7a, Wnt7b, Wnt9a, and
101 Wnt11 are expressed in the developing cochlear epithelium and Wnt5a is expressed in
102 both the cochlear epithelium and periotic mesenchyme (POM)[15, 26, 27]. Wnt7a mutant
103 cochleae show normal hair cell orientation[28]. While Wnt5a knockout cochleae display
104 defects in convergent extension, hair cell orientation, and localization of Vangl2, although
105 the defects were minor and penetrance was limited, with only one third of mutants
106 affected[29]. We and others have previously shown that concurrent ablation of Wnt
107 members in the cochlear epithelium (by deleting Wntless or Wnt5a and Wnt7b) caused a
108 significant shortening of the cochlea, mild misorientation of hair cells, and mislocalization
109 of a subset of core PCP proteins (Fzd6 and Dvl2) in hair cells[15, 30, 31]. Because the severity
110 of hair cell polarity defects observed in these studies is relatively mild in comparison to

111 other PCP mutants (e.g., Vangl2-looptail[16]), the requirement of Wnts for PCP signaling I
112 the cochlea has remained controversial[32, 33].
113 Here, we used computational analysis of single-cell transcriptomic data from the
114 developing cochlea and identified Wnt5a, Wnt7a, and Wnt7b in the cochlear epithelium
115 and Wnt5a in the surrounding POM as the top candidate Wnts that act on developing hair
116 cells. Deletion of multiple Wnts (Wnt5a, Wnt7a, and Wnt7b) from the cochlear epithelium
117 shortened the cochlear duct, without causing misorientation of hair cells or mislocalization
118 of core PCP proteins, suggesting a redundancy among Wnts. Inhibiting the secretion of
119 both epithelial and mesenchymal Wnts further shortened the cochlea and led to severely
120 malrotated hair cells and loss of polarization of all PCP proteins examined, with
121 phenotypes remarkably more severe than Wntless ablation in the cochlear epithelium
122 alone. Collectively, our study indicates that multiple secreted Wnts from both the epithelial
123 and mesenchymal compartments are required for cochlear outgrowth, hair cell orientation
124 and PCP signaling.
125
126 **Results**
127 **Ablating Wntless from the cochlear epithelium disrupts cochlear outgrowth and**
128 **hair cell polarization.**
129 Wntless (Wls) is a chaperone transmembrane protein required for secretion of Wnt
130 proteins, a process essential for all Wnts[34, 35]. We found that Wntless mRNA is expressed
131 throughout the developing cochlear epithelium (Fig. 1b, Supplementary Fig. 1c-c", e-e",
132 g-g"), corroborating previous results[15]. To ablate Wntless in the cochlear epithelium prior
133 to hair cell differentiation, we first established Emx2-Cre; Wls-flox mice. Emx2-Cre activity

134 starts in the otocyst as early as embryonic (E) 10.5 (Fig. 1a)[36]. In E16.5 *Emx2*$^{Cre/+}$;
135 *Wls*$^{flox/flox}$ (Emx2-Wls cKO) cochleae, there was almost no detectable Wls mRNA in the
136 cochlear epithelium, whereas that in the POM remained comparable to those in control
137 cochleae (Fig. 1c, Supplementary Fig. 1d-d", f-f", h- h"), indicating efficient and specific
138 deletion of Wls within the cochlear epithelium in Emx2-Wls cKO mice. At E18.5, Emx2-
139 Wls cKO cochleae are significantly shorter (~39%) than those from wildtype littermates
140 (2,856±381 and 4,653±220 μm, respectively, $p < 0.0001$) (Fig. 1d, e). Moreover, Emx2-
141 Wls cKO cochleae displayed significantly fewer (~29%) Myosin7A-positive hair cells
142 (mean 1,917±234 and 2,692±156 per cochlea, respectively, $p < 0.01$, Fig. 1f). These
143 findings suggest that inhibiting Wnt secretion in the cochlear epithelium leads to defects
144 in cochlear outgrowth and/or convergent extension. To assess hair cell orientation in
145 phalloidin-stained E18.5 cochleae (Fig. 1g, h, Supplementary Fig. 1i, j), we measured the
146 average and variability of orientation of each row of hair cells (circular mean and variance).
147 In control mice at E18.5, cochlear hair cell bundles face laterally with the most lateral row
148 of hair cells (the third row of OHCs) slightly rotated toward the apex (Fig. 1g-g',
149 Supplementary Fig. 1i-i'), consistent with previous reports[28, 37]. Compared to controls,
150 Emx2-Wls cKO cochlear hair cells exhibited significantly larger variance in the middle and
151 basal turns (circular variance ratio: 2.00, Supplementary Table 1), along with a mild, but
152 significantly different mean orientation of HCs (IHC, OHC1, and OHC3+, Fig. 1h-h', i,
153 Supplementary Fig. 1j-j', k, Supplementary Table 1). We also examined the molecular
154 basis of cochlear PCP by assessing the polarized expression of core PCP proteins in hair
155 cells. Hair cells display a complement of core PCP proteins[15] (Fig. 1j). In the control
156 cochlea, we found Fzd6, Vangl2, and Celsr1, to be localized to the medial junctions and

157 Dvl2 to the lateral junctions of OHCs (Fig. 1k-k''', m, o). By contrast, the Emx2-Wls cKO
158 cochlea lacked polarized expression of Fzd6 and Dvl2 while Celsr1 and Vangl2 remained
159 polarized (Fig. 1l-l''', n, p). This finding suggests that Wnt secretion from the cochlear
160 epithelium is required for establishing and/or maintaining the polarization expression of a
161 subset of, but not all, core PCP proteins. Taken together, our data suggest that disruption
162 of Wnt secretion from the cochlear epithelium prevents elongation of the organ and
163 causes a mild PCP defect (shortened cochlea, hair cell misorientation, and loss of
164 polarized expression of a subset of PCP proteins), corroborating previous reports[15, 31].
165

166 ***In silico* analysis identified candidate Wnt ligands from the cochlear epithelium and**
167 **periotic mesenchyme regulating planar cell polarization**

168 To identify candidate Wnt ligands in the developing cochlea that could contribute
169 to hair cell polarity, we analyzed established single-cell transcriptomic data from the
170 embryonic cochleae. We integrated existing single-cell RNA sequencing data into two
171 categories, each comprised of both epithelial and mesenchymal cells: (1) early (E13.5
172 and E14.5)[38, 39] and late embryonic cochlea (E15.5 and E16.5)[39, 40]. From the analysis of
173 both the early and late embryonic cochlea datasets, we identified six cell clusters: hair
174 cells (HCs), cochlear roof, lesser epithelial ridge (LER), greater epithelial ridge (GER),
175 pro-sensory cells, and periotic mesenchyme cells (POM). These clusters were annotated
176 using previously described marker genes[39, 40].

177 We next computationally inferred cell-cell communication among different cell
178 clusters with a focus on Wnt ligand-receptor interactions in the developing cochlea using
179 the CellChat[41] algorithm. First, we combined the cochlear epithelial cells (cochlear roof,

180 LER, and GER cells), while excluding hair cells and prosensory cells. As a result, we
181 generated four new cell groups for the early and late embryonic cochlea datasets: 1) the
182 “Epithelial cells” group (comprising cochlear roof, LER, and GER cells); 2) the “POM”
183 group; 3) the “Prosensory cells” group; and 4) the “Hair cells” group, which includes both
184 IHCs and OHCs (Fig. 2a, b). We then used these newly defined cell groups to create
185 circle plots for each dataset, illustrating significant Wnt-receptor interactions among the
186 cell groups, with the width of the arrows reflecting the scale of these interactions based
187 on the calculated communication probability (Fig. 2c, d)[41]. In the early embryonic cochlea
188 dataset, significant bidirectional Wnt ligand-receptor interactions were detected among
189 all cell groups, along with autocrine signaling (Fig. 2c). In contrast, in the late embryonic
190 cochlea dataset, outgoing Wnts from the hair cell group interacting with any other group
191 were no longer significant (Fig. 2d). Furthermore, in both datasets, the strength of Wnt
192 ligand-receptor interactions involving the POM group was particularly notable (Fig. 2c, d).
193 To identify the Wnt subtype received by the hair cell and prosensory/supporting cell
194 groups, we analyzed the Wnt-ligand interactions in which these cells act as receptors and
195 created chord plots illustrating the significant Wnt ligand-receptor pairs for each dataset
196 (Fig. 2e, f). The values for the relative contribution, reflecting the calculated
197 communication probability of each Wnt ligand-receptor (Source data 1), and are
198 proportional to the width of the lines in the chord plots (Fig. 2e, f). We then categorized
199 and ranked the candidate Wnt ligands received by the hair cell and prosensory/supporting
200 cell groups separately based on whether they originate from the cochlear epithelium or
201 POM (Fig. 2g-j). In the early embryonic cochlea dataset, Wnt7b was identified as the
202 dominant Wnt from the cochlear epithelium, followed by Wnt7a and Wnt5a. In contrast,

203 for the late embryonic cochlea dataset, Wnt5a emerged as the dominant candidate Wnt
204 from the cochlear epithelium, followed by Wnt7b and Wnt7a (Fig. 2g, h). Among the Wnts
205 derived from the POM, Wnt5a was the most highly expressed across both datasets, with
206 Wnt5b following (Fig. 2i, j). In summary, the cell-cell communication analysis of both
207 datasets suggests Wnt5a, Wnt7a, and Wnt7b as candidate Wnts secreted from the
208 cochlear epithelium, with Wnt5a being the most robust among those derived from the
209 POM, that can contribute to Wnt signaling in hair cells during cochlear development.
210

211 **Deletion of Wnt5a, Wnt7a, and Wnt7b from the cochlear epithelium shortens**
212 **cochlea and causes mild hair cell malrotation.**

213 Because our computational analysis identified Wnt5a, Wnt7a, and Wnt7b as the
214 candidate Wnt ligands in the cochlear epithelium acting on hair cells and prosensory cells,
215 we hypothesized that concurrent deletion of these Wnt ligands from the cochlear
216 epithelium would phenocopy Emx2-Wls cKO cochlea. To test this hypothesis, we crossed
217 conditional KO animals of Wnt5a[42], Wnt7a[43], or Wnt7b[44] with Emx2-Cre mice, and
218 generated *Emx2*$^{Cre/+}$*; Wnt5a*$^{flox/flox}$ (Emx2-Wnt5a cKO), *Emx2*$^{Cre/+}$*; Wnt7a*$^{flox/flox}$ (Emx2-
219 Wnt7a cKO), and *Emx2*$^{Cre/+}$*; Wnt7b*$^{flox/flox}$ (Emx2-Wnt7b cKO) mice. Previous studies
220 using *in situ* hybridization have demonstrated the expression of Wnt5a, Wnt7a, and
221 Wnt7b in the cochlear epithelium, particularly on the cochlear floor, at E14.5 and E16.5[15,
222 28, 29] (Fig. 3a). In E16.5 control cochlea, we confirmed expression of Wnt5a, Wnt7a, and
223 Wnt7b mRNA (Supplementary Fig. 2a, c, e, g, i, k), which were mostly deleted in the
224 cochlear epithelium of the Emx2-Wnt5a, Emx2-Wnt7a, and Emx2-Wnt7b cKO mice
225 (Supplementary Fig. 2b, d, f, h, j, l).

226 When Wnt5a, Wnt7a, or Wnt7b was individually ablated in the cochlear epithelium,
227 there was no significant difference in cochlear length compared to littermate controls (p =
228 0.5132, 0.9070, and 0.4882, respectively; Supplementary Fig. 3a-b, f-g, k-l). Additionally,
229 hair cell counts in these Emx2-Wnt5a and Emx2-Wnt7a cKO cochleae were unchanged
230 (p = 0.5722 and p = 0.5056, respectively), whereas Emx2-Wnt7b cKO cochleae had
231 mildly reduced hair cell counts (~9%; $p < 0.05$, Supplementary Fig. 3c, h, m). Furthermore,
232 the circular mean and variance of hair cell orientation in Emx2-Wnt5a and Emx2-Wnt7a
233 cKO cochleae were comparable to controls, while those in Emx2-Wnt7b cKO cochlea
234 were mildly abnormal (significant deviation of IHC, OHC1 and OHC2, Supplementary Fig.
235 4a-r, Supplementary Table 1). Lastly, Fzd6 and Dvl2 remained polarized in OHCs of
236 Emx2-Wnt5a, Emx2-Wnt7a, and Emx2-Wnt7b cKO cochleae (Supplementary Figure 3d-
237 e''', i-j''', n-o'''). These findings suggest that individual deletion of Wnt5a, Wnt7a, or Wnt7b
238 from the cochlear epithelium during development has a minimal effect on cochlear
239 extension and hair cell polarization, corroborating previous reports[15, 30].
240 Previously, Wnts were reported to have redundant functions during cochlear
241 development[30, 45]. To rule out this possibility, we generated double KO mice for Wnt
242 ligands: *Emx2*$^{Cre/+}$; *Wnt5a*$^{flox/flox}$; *Wnt7a*$^{flox/flox}$ (Emx2-Wnt5a; Wnt7a cKO), *Emx2*$^{Cre/+}$;
243 *Wnt5a*$^{flox/flox}$; *Wnt7b*$^{flox/flox}$ (Emx2-Wnt5a; Wnt7b cKO), and *Emx2*$^{Cre/+}$; *Wnt7a*$^{flox/flox}$;
244 *Wnt7b*$^{flox/flox}$ (Emx2-Wnt7a; Wnt7b cKO) mice. The cochlear length of Emx2-Wnt5a;
245 Wnt7b and Emx2-Wnt7a; Wnt7b cKO, but not Emx2-Wnt5a; Wnt7a cKO, mice were
246 significantly shorter than those of littermate controls (~20% and ~24%, $p < 0.01$ and $p <$
247 0.05, respectively) (Supplementary Fig. 5a-b, f-g, k-l). Hair cell counts in Emx2-Wnt5a;
248 Wnt7b and Emx2-Wnt7a; Wnt7b cKO cochleae were significantly lower than controls

249 (~20% and ~15%, $p < 0.01$ and $p < 0.05$, respectively), whereas hair cell counts in Emx2-
250 Wnt5a; Wnt7a cKO cochleae were comparable to littermate control cochleae ($p = 0.6008$,
251 Supplementary Fig. 5c, h, m). Emx2-Wnt5a; Wnt7a cKO cochleae showed normal hair
252 cell orientation (Supplementary Fig. 6a-f, 13), while Emx2-Wnt5a; Wnt7b cKO cochleae
253 exhibited more variable orientation of hair cells compared to controls (circular variance
254 ratio: 1.73, Supplementary Table 1). However, the average orientation of hair cells in
255 Emx2-Wnt5a; Wnt7b cKO cochleae were not significantly different from controls
256 (Supplementary Fig. 6g-r, 13, Supplementary Table 1). Hair cells in all three double cKO
257 cochleae still exhibited polarized expression of Fzd6 and Dvl2 (Supplementary Fig. 5d-
258 e''', i-j''', n-o'''), in contrast to the previously reported reduced expression in Emx2-Wnt5a;
259 Wnt7b cKO cochleae[30].

260 Finally, we generated and examined the *Emx2*$^{Cre/+}$; *Wnt5a*$^{flox/flox}$; *Wnt7a*$^{flox/flox}$;
261 *Wnt7b*$^{flox/flox}$ (Emx2-Wnt5a; Wnt7a; Wnt7b cKO) mice. In these animals, cochlear length
262 was significantly lower than that of littermate controls (~30%, $p < 0.001$; Fig. 3b, c), and
263 that after concurrent deletion of Wnt5a and Wnt7a ($p < 0.0001$, Fig. 3e). Length of Emx2-
264 Wnt5a; Wnt7a; Wnt7b cKO cochlea is comparable to that of Emx2-Wnt5a; Wnt7b cKO,
265 Emx2-Wnt7a; Wnt7b cKO, and Emx2-Wls cKO cochleae ($p > 0.05$ for all, Fig. 3e). Hair
266 cell counts of Emx2-Wnt5a; Wnt7a; Wnt7b cKO cochleae were significantly reduced
267 compared to littermate controls (~16% and $p < 0.01$; Fig. 3d). Similarly, hair cell counts in
268 Emx2-Wnt5a; Wnt7a; Wnt7b cKO cochleae were significantly lower than those in any
269 single cKO (~17% and $p < 0.01$ for Wnt5a cKO, ~18% and $p < 0.01$ for Wnt7a cKO, and
270 ~14% and $p < 0.05$ for Wnt7b cKO cochleae) or Emx2-Wnt5a; Wnt7a cKO cochleae
271 (~15% $p < 0.05$), yet comparable to those in Emx2-Wnt5a; Wnt7b cKO, Emx2-Wnt7a;

272 Wnt7b cKO, and Emx2-Wls cKO cochleae at E18.5 ($p > 0.05$ for all, Fig. 3f). These results
273 suggest that Wnt5a, Wnt7a, and Wnt7b in the cochlear epithelium are individually
274 dispensable yet contribute additively to cochlear outgrowth. By contrast, no misorientation
275 of the hair cells was detected (basal or middle turns) (Fig. 3g-i, Supplementary Fig. 7a-c,
276 Supplementary Table 1). Furthermore, Fzd6 and Dvl2 expression in hair cells remains
277 polarized (Fig. 3j-k'''). While the length of Emx2-Wnt5a; Wnt7a; Wnt7b cKO is similar to
278 that of Emx2-Wls cKO, hair cell orientation and core PCP protein expression were
279 remarkably normal.

280 In summary, these data indicate that the effects of Wnt5a, Wnt7a, and Wnt7b from
281 cochlear epithelium are additive for cochlear outgrowth, but not for hair cell orientation.
282 Furthermore, since core PCP protein expression remains polarized in all single, double,
283 and triple conditional KO cochleae, we postulate that additional Wnt ligands, either within
284 or outside the cochlear epithelium, may also contribute to planar polarization.

285

286 **Deletion of Wnt5a from the POM does not cause cochlear PCP defects.**

287 Our computational cell-cell communication analysis inferred that Wnt ligands from
288 the POM significantly interact with Wnt receptors on hair cells and prosensory/supporting
289 cells, particularly Wnt5a (Fig. 2e, f, i, j). Indeed, a previous study has reported Wnt5a
290 expression in the POM at E14.5[46]. To test the hypothesis that Wnt ligands from the POM
291 regulate cochlear outgrowth and hair cell polarity, we generated *Dermo1 (Twist2)-Cre;*
292 *Wls*$^{flox/flox}$ mice. Dermo1-Cre mice exhibit Cre activity beginning around E9.5 in the
293 mesenchyme-derived tissues[47], including the POM but not the cochlear epithelium[48].
294 However, *Dermo1*$^{Cre/+}$*; Wls*$^{flox/flox}$ (Dermo1-Wls cKO) were embryonically lethal (8 of 8

295 animals by E18.5) as previously reported,[49] precluding examination of their cochlea. We
296 next generated and examined *Dermo1*$^{Cre/+}$; *Wnt5a*$^{flox/flox}$ (Dermo1-Wnt5a cKO) mice. In
297 control cochleae, Wnt5a mRNA was detected both in the cochlear epithelium and POM
298 (Fig. 4b-b', Supplementary Fig. 8a-a', c-c'), corroborating our previous study[15]. By
299 contrast, in Dermo1-Wnt5a cKO cochleae, *Wnt5a* mRNA signals in the POM were
300 undetectable while those in other regions (cochlear epithelium and spiral ganglion)
301 remained present (Fig. 4c-c', Supplementary Fig. 8b-b', d-d'), indicating efficient and
302 specific deletion of Wnt5a mRNA from the POM. For the cochlear PCP readouts, however,
303 Dermo1-Wnt5a cKO cochleae exhibited normal length, hair cell counts, hair cell
304 orientation (both circular variance and means), and polarized expression of the core PCP
305 proteins Fzd6 and Dvl2 (Fig. 4d-k''', Supplementary Fig. 8e-g, Supplementary Table 1).
306 These results suggest that deletion of Wnt5a alone from the POM does not disrupt
307 cochlear outgrowth, hair cell orientation and PCP signaling.
308
309 **Inhibition of Wnt secretion in both the cochlear epithelium and periotic**
310 **mesenchyme causes severe planar polarization defects.**
311 When Wnt secretion was prevented in the cochlear epithelium using Emx2-Wls
312 cKO mice, we have shown that hair cell orientation and polarization of two core PCP
313 proteins were disrupted, albeit to a markedly milder degree relative to other PCP
314 mutants[10, 12] (Fig. 1g-i, Supplementary Fig. 1i-k). Since Wnts from both the cochlear
315 epithelium and POM were predicted to significantly interact with Wnt receptors on hair
316 cells and prosensory/supporting cells (Fig. 2g-q), we generated *Sox9*^{CreERT2}; *Wls*$^{flox/flox}$
317 (Sox9-Wls cKO) mice to prevent Wnt secretion in both regions. Sox9 is expressed in both

318 the otic/cochlear epithelium and POM from E9.5 to E14.5, before becoming more
319 restricted later[50, 51]. Sox9-Wls cKO animals received tamoxifen (0.2 mg/g of body weight)
320 at E10.5-11.5 or E11.5-12.5 with survival rates of ~73% at E18.5, consistent with previous
321 reports[52, 53] (n=48, Fig. 5a, Supplementary Fig. 9a). In E18.5 Sox9-Wls cKO cochlea, we
322 found efficient and broad deletion of Wls in both the cochlear epithelium and POM
323 (Supplementary Fig. 10a- f').

324 After tamoxifen administration at E10.5-11.5, Sox9-Wls cKO cochleae were
325 dramatically shorter and contained significantly fewer hair cells than controls (~70% and
326 ~60%, $p < 0.0001$ for both, Fig. 5b-d) and Emx2-Wls cKO cochleae (~38% and $p < 0.0001$,
327 and ~46% and $p < 0.01$, respectively). Sox9-Wls cKO cochlea displayed five to six rows
328 of hair cells throughout the cochlea (Fig. 5e-f, Supplementary Fig. 11a-b), consistent with
329 a defect in convergent extension seen in PCP mutants[54, 55]. Additionally, hair cells
330 appeared disorganized without a clear separation between IHCs and OHCs (Fig. 5f,
331 Supplementary Fig. 11b), possibly suggesting abnormal pillar cell development.
332 Furthermore, hair cells were severely malrotated with significantly higher variance and
333 more deviation than controls (circular variance ratio: 5.33, Fig. 5e-g, Supplementary Fig.
334 11a-c, Supplementary Table 1). Unlike Emx2-Wls cochleae, where only a subset of hair
335 cells was significantly malrotated and directed to the base, Sox9-Wls cochleae shows that
336 each row of hair cells is severely malrotated (Fig. 1g-i, 4e-g, Supplementary Fig. 1i-k,
337 11a-c, Supplementary Table 1). In contrast to PCP mutants where hair cells are randomly
338 malrotated[12, 16, 17], Sox9-Wls cochlear hair cells are rotated towards the apex, suggesting
339 a global instructive role for secreted Wnts.

340 In control cochleae, Celsr1, Vangl1, Vangl2, and Fzd6 are localized to the medial
341 junctions of hair cells, while Dvl2 is found at the lateral junctions (Fig. 5h, j, l, n, p). In
342 contrast, each of these core PCP proteins is mislocalized in hair cells in Sox9-Wls cKO
343 cochleae (Fig. 5i, k, m, o, p). Overall, compared to Emx2-Wls cKO cochleae, Sox9-Wls
344 cKO mice exhibited greater disruptions in cochlear duct elongation, hair cell orientation,
345 and polarization of core PCP proteins in hair cells.

346 To determine whether the reduced length and hair cell counts in Sox9-Wls cKO
347 cochleae were attributed to reduced proliferation, we performed Ki67 immunostaining and
348 EdU labeling. EdU (50 mg/kg, IP) was administered at E12.5, along with tamoxifen (0.2
349 mg/g) at E10.5-11.5. At E15.5, both control and Sox9-Wls cKO cochleae displayed Ki67-
350 positive and EdU-positive cells in both the cochlear epithelium and POM (Fig. 5r-s). No
351 significant difference was observed in the number of EdU- or Ki67-labeled Sox2-positive
352 cells in control and Sox9-Wls cKO cochleae ($p = 0.1015$ and $p = 0.4776$, respectively; Fig.
353 5t-u, Supplementary Fig. 11d-e). Additionally, no significant differences were detected in
354 the number of EdU- or Ki67-positive cells in the POM ($p = 0.7144$ and $p = 0.4975$,
355 respectively; Fig. 5r-s, Supplementary Fig. 11d-e). These findings suggest that the
356 cochlear shortening and reduced cochlear hair cell counts observed in Sox9-Wls cKO
357 mice are primarily due to disruptions in cochlear outgrowth and/or convergent extension.

358 To determine whether the regulation of cochlear outgrowth and PCP development
359 by Wnt secretion is time-dependent during cochlear development, we ablated Wntless
360 one day later (tamoxifen at E11.5-12.5, Supplementary Fig. 9a). Sox9-Wls cKO cochleae
361 were still significantly shorter (~26% and $p < 0.05$) and contained fewer hair cells (~14%
362 and $p < 0.05$) compared to controls at E18.5 (Supplementary Fig. 9b-d). However, when

363 compared an earlier injection of tamoxifen at E10.5-11.5, both the cochlear length (~60%
364 and $p < 0.0001$) and hair cell counts (~53% and $p < 0.0001$) were significantly higher
365 (Supplementary Fig. 9c-d). Additionally, hair cells remain significantly malrotated towards
366 the apex and showed a high variance in orientation (circular variance ratio: 3.28,
367 Supplementary Fig. 9e-j, Supplementary Table 1). However, core PCP proteins (Fzd6,
368 Celsr1, Vangl1, and Vangl2) were all polarized in hair cells (Supplementary Fig. 9k-s),
369 suggesting the overall effects were less severe than Wntless deletion earlier. These
370 results suggest that the effect of Wnts on the cochlear PCP development is highly time-
371 sensitive during the embryonic period.

372 Overall, these data suggest that secreted Wnt proteins, around E10.5-11.5, from
373 both the POM and cochlear epithelium are required for elongation of the cochlear duct,
374 orientation of hair cells, and polarization of core PCP proteins in hair cells during cochlear
375 development.

376

377 **Discussion**

378 During development, the mouse cochlea elongates to form a spiral organ that is
379 two and a half turns in length, in which sensory and non-sensory cells differentiate and
380 undergo precise radial patterning. These steps are temporally and spatially coordinated
381 and governed by the Notch, Wnt, and Shh signaling pathways[2]. PCP signaling critically
382 regulates cochlear elongation and sensory cell polarization. Previous studies have shown
383 that secreted Wnts in the cochlear epithelium are required for cochlear elongation,
384 sensory cell polarization, and polarization of PCP proteins[15, 31], although the severity of
385 the sensory cell polarization defects was remarkably mild, raising the possibility that other

386 factors co-regulate these steps. Here, based on computational analysis of single-cell
387 transcriptomes of the developing cochlear epithelium and surrounding POM, we predicted
388 that Wnt5a, Wnt7a and Wnt7b in the cochlear epithelium, and Wnt5a in the POM were
389 the most potent Wnts acting on the developing hair cells and prosensory/supporting cells.
390 Using combinations of transgenic mice, we selectively deleted Wnt members or Wnt
391 secretion in a spatiotemporally selective manner. We first demonstrated that these Wnt
392 members in both the cochlear epithelium and POM additively contribute to cochlear
393 outgrowth and convergent extension. By contrast, hair cell orientation and PCP signaling
394 based on the polarized expression of core PCP proteins are only mildly affected despite
395 deletion of all three Wnt members or Wntless in the cochlear epithelium. When Wnt
396 secretion was prevented in both the cochlear epithelium and POM, cochlear length, hair
397 cell orientation and PCP signaling were severely affected, suggesting that Wnt members
398 distributed across the epithelial and mesenchymal compartments are highly redundant in
399 regulating cochlear development.
400
401 Wnts are required for cochlear hair cell planar cell polarity and cochlear outgrowth
402 In our current study, inhibition of Wnt secretion in the cochlear epithelium during
403 development only caused mild hair cell misorientation and loss of polarization in a subset
404 of core PCP proteins, consistent with previous studies[15, 31]. This suggests that Wnt
405 proteins from the cochlear epithelium have a limited role in establishing hair cell polarity.
406 In contrast, Sox9-Wls cKO cochleae demonstrated severe hair cell misorientation and
407 loss of polarization of all core PCP proteins examined. Thus, Wnts from both the cochlear
408 epithelium and POM are critical in regulating hair cell polarity.

409 Wnts have previously been implicated to function as global cues for PCP[25]. In
410 Drosophila, Wingless and Wnt4 modulate intercellular Fzd–Vangl interactions, thereby
411 establishing directional cues for PCP axis orientation[56]. However, recent studies in
412 Drosophila have challenged the idea that secreted Wnts are required for core PCP protein
413 enrichment and planar polarity[57, 58]. In various vertebrate organs, the role of Wnt ligands
414 in regulating PCP is well established. For instance, Wnt5b and Wnt11 coordinate cardiac
415 remodeling through polarization of actomyosin activity in zebrafish. During chick muscle
416 development, Wnt11 directs elongation of myocytes along the antero-posterior axis of the
417 embryo[59]. In mice, Wnt5a establishes PCP in limb mesenchyme[60, 61] and Wnt5a and
418 Wnt5b direct node cell polarization in the developing heart[62], while Wnt5a induces
419 phosphorylation of Vangl2 in a dose-dependent manner[63]. However, the relationship
420 between Wnt signaling and PCP is not yet clear in the cochlea.

421 In the mouse cochlea, several studies have found that Wnt proteins in the cochlear
422 duct regulate the orientation and PCP signaling in hair cells[15, 30, 31]. However, in part
423 because deficiency of Wnt proteins results in hair cell defects that are relatively mild
424 compared to other PCP mutants, it has been suggested that Wnts do not play a central
425 role in determining cochlear PCP[32, 33]. Our results in this study clearly show that both
426 epithelial and mesenchymal Wnts contribute to cochlear outgrowth and hair cell planar
427 cell polarity, and not merely epithelial Wnts as previously suggested[15, 30, 31].

428 PCP mutants such as *Vangl2*$^{Lp/Lp}$ demonstrate convergent extension defects, with
429 shorter cochleae (~27% of wild-type littermates) without a significant reduction of hair
430 cells[10]. In contrast, ablation of Wntless in the cochlear epithelium (Emx2-Wls cKO) and in
431 both the cochlear epithelium and POM (Sox9-Wls cKO) lead to significantly shorter

432 cochleae (~38% and 70%, respectively) and a decrease in hair cells. Because the degree
433 of shortening is severe and more than accounted for by the convergent extension defect
434 alone, our study suggests that both epithelial and POM Wnt proteins are required for
435 cochlear outgrowth and convergent extension. When comparing the results from
436 transgenic mouse lines to delete one or multiple Wnts and epithelial or both epithelial and
437 mesenchymal Wnts, we conclude that multiple Wnt members additively contribute to
438 cochlear outgrowth (Fig. 6).

439 While cochlear PCP mutants are characterized by hair cell malrotation, different
440 degrees of defects have been reported, with Vangl2 and Celsr1 mutants being more
441 severe and the Vangl1 mutant milder[16, 17]. Moreover, core PCP proteins serve redundant
442 functions, with deletion of multiple members or the presence of the dominant negative
443 Vangl2-looptail mutation accentuating the polarity defects[12, 14, 16]. Several studies have
444 demonstrated that deletion of Wntless or multiple Wnts in the cochlear epithelium causes
445 mild hair cell polarity defects and loss of or decreased polarized expression of Fzd6 and
446 Dvl2, but not other core PCP proteins. When Wnt secretion is prevented in both cochlear
447 epithelium and periotic mesenchyme (using Sox9-Wls cKO at E10.5-11.5 and not E11.5-
448 12.5), hair cell polarity defects are severe and all core PCP proteins mislocalized. Thus,
449 our study demonstrates that secreted Wnt proteins are not only required for PCP
450 establishment in the developing cochlea (hair cell orientation and core PCP localization)
451 but also do so in an additive and time-dependent manner.

452

453 <u>Dual regulation of hair cell orientation by PCP core proteins and Wnts</u>

454 Cochlear hair cells are uniformly oriented with their bundles facing laterally. Prior
455 work on PCP mutants has characterized hair cell orientation to be highly variable with
456 random rotation in both clockwise and counterclockwise directions[10, 12, 17]. These results
457 suggest a local, instructive role for core PCP proteins in guiding the polarization of hair
458 cells and limiting variance in orientation. In support of this role, Vangl2 misexpression
459 increases the variance of hair cell orientation without affecting the average angle of their
460 rotation in the chicken basilar papilla[64].

461 The role of Wnt ligands in regulating hair cell orientation and PCP is less clear, as
462 Wntless deletion in the cochlear epithelium increases variance in hair cell orientation
463 without significantly affecting the average position, suggesting also a local instructive
464 role[15]. However, in the presence of the Vangl2-looptail mutation, Wntless deletion in the
465 cochlear epithelium leads to malrotation of hair cells towards the apex, suggesting that
466 Wnt ligands in the epithelium may serve as an instructive global cue[15]. In a similar vein,
467 inhibition of endogenous Wnts by inhibitors Sfrp1 or Wif1 in cultured mouse cochlea
468 directed hair cells to uniformly rotate unidirectionally[28]. In the current study, deletion of
469 Wls from both the cochlear epithelium and POM resulted in pronounced and uniform hair
470 cell rotation toward the apex, further supporting the notion that Wnt proteins provide an
471 instructive global cue for hair cell orientation. Together, we propose a model where hair
472 cell orientation and cochlear outgrowth are regulated by both core PCP proteins and Wnt
473 proteins from the epithelial and mesenchymal compartments in the developing cochlea.
474 In the model, core PCP proteins serve local instructive roles while Wnt proteins play a
475 more global role in guiding cell and tissue organization (Fig. 6).

476 In *Vangl2*$^{Lp/Lp}$ and other PCP mutants, hair cell malrotation is most severe in the
477 lateral-most most hair cells (i.e., abneural OHC3+), but the direction of malrotation is
478 random[10]. After broad Wntless deletion (Sox9-Wls cKO), hair cell malrotation is also most
479 severe in the lateral-most hair cells (Supplementary Table 1), but malrotation is almost
480 exclusively directed towards the apex. Hair cell malrotation towards the apex is also
481 observed in Emx2-Wls cKO in the presence of the *Vangl2*$^{Lp/+}$ allele[15], suggesting that
482 Wnts may act as a global instructive cue for hair cell orientation. It is possible that other
483 signaling pathways also contribute to cochlear patterning. For example, Wnt and FGF
484 signaling are both crucial in maintaining migratory polarity and gene expression domains
485 in the lateral line primordium in zebrafish[65] and regulating PCP during mouse limb
486 development[61]. Lastly, it is also possible that local shearing forces organize and pattern
487 hair cells and supporting cells differentially along the abneural-neural axis[32, 66].
488
489 <u>Wnt ligand-receptor interaction between epithelial and mesenchymal tissues</u>
490 Our study suggests that Wnt proteins from both the epithelium and POM regulate
491 the development of PCP in the cochlear epithelium. While Wnt ligands are classically
492 thought to act at short to medium ranges, they have been shown to travel remarkable
493 distances to mediate mesenchymal-epithelial crosstalk in other organ systems. For
494 example, Wnt9b in the Wolffian duct epithelium also regulates the development of
495 metanephric mesenchyme and mesenchymal to epithelial transitions[67]. Also,
496 mesenchymal cells secrete Wnt proteins to regulate stem cell proliferation and
497 differentiation in both the intestines and airway[68, 69, 70]. These studies illustrate the Wnt-
498 mediated mesenchymal-epithelial crosstalk during tissue development and homeostasis.

499 The distance and mechanisms by which Wnts are transported are likely context-
500 dependent[71, 72, 73], and warrants investigation given their significant roles in cochlear
501 development.
502
503 Many Wnt members contribute to cochlear development
504 Among the seven Wnt members expressed in the developing cochlea, our
505 computational cell-cell communication analysis predicts Wnt5a, Wnt7a, Wnt7b as the
506 most potent ligands to interact with corresponding receptors on hair cells. We and others
507 have found robust expression of Wnt5a mRNA in the cochlear epithelium flanking the
508 organ of Corti and the periotic mesenchyme from E12.5 to E16.5, higher in the base than
509 the apex[15, 30]. On the other hand, Wnt7a and Wnt7b mRNA are both broadly expressed
510 in the cochlear duct with no apparent apical-basal gradient. In agreement with prior
511 studies[15, 30], deletion of both Wnt5a and Wnt7b in the cochlear duct leads to significant
512 shortening of the cochlear duct and mild hair cell orientation defects. However, either
513 deletion alone has a minimal effect. Interestingly, deletion of both Wnt7a and Wnt7b in
514 the cochlear duct shortens the cochlea to the extent similar to that of deletion of
515 Wnt5a/Wnt7b, supporting the notion that Wnt proteins additively regulate cochlear
516 outgrowth. As Emx2-Wls cKO cochleae display more severe PCP defects than Emx2-
517 Wnt5a; Wnt7a; Wnt7b cochleae, we attribute this to either Wnt redundancy or incomplete
518 deletion in the latter model. Four other Wnt members (Wnt4, Wnt9a, Wnt11, and Wnt2b)
519 are also expressed at low levels in the developing cochlear duct[15] and may also contribute
520 to hair cell PCP signaling. According to our cell-cell communication computational
521 analysis, Wnt5a is deemed the most potent Wnt ligand; however, neither deletion of

522 Wnt5a in the POM (DermoCre-Wnt5a cKO) nor in the cochlear duct alone[15] causes
523 cochlear shortening or hair cell misorientation.
524
525 Wnt signaling is not required for hair cell formation
526 Our data demonstrate that even though we deleted Wnts or Wls either in the
527 cochlear epithelium or in both the cochlear epithelium and POM, hair cell formation still
528 occurs. This data suggests that secreted Wnts are not required for hair cell formation after
529 E10.5. Previous *in vivo* mouse studies deleting beta-catenin, the central mediator of
530 canonical Wnt signaling, show conflicting results. In mice where conditional deletion of
531 beta-catenin was performed using the CMV-CreER allele (tamoxifen at E11.5), Atoh1+
532 hair cells were absent at E14.5[21]. However, hair cells were observed at later time points
533 (E15.5-18.5) when other mouse lines were examined (Sox2-CreERT2 (tamoxifen at E12
534 or E13), Fgf20-Cre, Emx2-Cre)[21, 23, 74]. Together with the current study, these results
535 suggest that neither beta-catenin nor secreted Wnts are required for cochlear hair cell
536 formation.
537
538 Summary
539 In conclusion, secreted Wnts from the cochlear epithelium and POM are essential for
540 establishing planar polarity in cochlear hair cells and for cochlear outgrowth during
541 development. Additionally, multiple Wnt ligands, including Wnt5a, Wnt7a, and Wnt7b,
542 contribute to cochlear outgrowth, hair cell orientation and PCP protein localization, to
543 ensure precise cochlear length and hair cell patterning.
544

545 **Materials and methods**

546 **Mice**

547 The following mouse strains were used; *Wls-flox*[75](#012888, Jackson laboratory, Bar
548 Harbor, ME), *Wnt5a-flox*[42] (Strain #026626), *Wnt7b-flox*[44](#008467), Sox9-CreERT2[76]
549 (#018829) (All from the Jackson Laboratory), *Wnt7a-flox*[43], Emx2-Cre[36], and
550 *Dermo1(Twist2)-Cre* mice [77]. All the floxed mouse lines for the Wnts above mentioned
551 are maintained by homozygous sibling matings, while *Emx2*$^{Cre/+}$ and *Dermo1*$^{Cre/+}$ mouse
552 lines are maintained by breeding heterozygous mice. Tamoxifen was administered
553 intraperitoneally to dams carrying the Sox9-CreERT2 allele at a dose of 200 µg/g. For the
554 EdU assay, a single dose (50 mg/kg; Invitrogen) was given via intraperitoneal injection to
555 pregnant mice at E12.5, and then cochlear tissue was collected at E15.5. Embryos were
556 considered E0.5 at noon on the day when a plug was discovered. The protocol is
557 approved by the Animal Care and Use Committee of Stanford University School of
558 Medicine (#18606).

559

560 **Genotyping**

561 DNA templates were generated by incubating tissues (ear punch or tail clipping) in 180 µl
562 of 50 mM NaOH at 98°C for 1 h followed by the addition of 20 µl of 1 M TrisHCl (pH 8.0).
563 We used either GoTaq® Master Mixes (M712) or KAPA2G Fast HotStart®
564 ReadyMix™(KK5609) to amplify DNA fragments. The primers used were: Wls-flox (fwd,
565 5′-aggcttcgaacgtaactgacc-3′; rev, 5′-ctcagaactcccttcttgaagc-3′), Wnt5a-flox (fwd, 5′-
566 ggtgagggactggaagttgc-3′; rev, 5′-ggagcagatgtttattgccttc-3′), Wnt7a-flox (fwd, 5′-
567 cacagccacccctagagagctcaatt-3′; rev, 5′-atgctttgccaggga acaccc-3′), Wnt7b-flox (fwd1, 5′-

568 gccagaggccacttgtgtag-3′; fwd2, 5′-ggtagtccttcctgcccttt-3′; rev, 5′-gtgtgtcctggcctgatttt-3′),
569 Emx2-Cre and Sox9-CreERT2 (fwd, 5′-gagtaatagcgaccaatcatcaagcc-3′; rev1, 5′-
570 cgaacatcttcaggttctgcgg-3′; rev2, 5′-cttggaagcgatgacccagatatcgg-3′), and Dermo1-Cre (wt
571 fwd, 5′-cgtctcagctacgccttctc-3′; wt rev, 5′-tcacgaggagagatacactgg-3′; mt fwd 5′-
572 aacttcctctcccggagacc-3′; mt rev, 5′-ccggttattcaacttgcacc-3′).
573

574 **Immunohistochemistry**

575 The heads of E15.5 or E18.5 mouse embryos were halved and fixed with 4%
576 paraformaldehyde (PFA, Electron Microscopy Sciences) in phosphate-buffered saline
577 (PBS, pH 7.4) for 2 hours for the following markers: Myosin7a, Sox2, Celsr1, Phalloidin,
578 Ki67, and DAPI. Fixation with 10% Trichloroacetic acid (TCA, Sigma-Aldrich, 1 hour on
579 ice) in Milli-Q water was performed for these markers: Frizzled-6 (Fzd6), Dishevelled-2
580 (Dvl2), Vangl1, Vangl2, and ZO-1. After fixation, all tissues were stored in PBS at 4°C.
581 For whole-mount preparation of E15.5 and E18.5 mouse cochlea, the otic capsule
582 was dissected from the fixed tissues, followed by the removal of the lateral wall. For
583 cochlear sections, fixed otic capsule was treated with 10%, 20%, and 30% sucrose in
584 PBS at 4°C for 1 hour, 1 hour, and overnight, respectively. The samples were then
585 embedded in OCT for cryosectioning at a thickness of 10 μm. Both the whole-mount preps
586 and sections were incubated with 0.1% Triton X-100 in PBS for 1 hour at room
587 temperature. Following this, the samples were blocked with 5% donkey serum, 0.1%
588 Triton X-100, 1% bovine serum albumin (BSA, #BP1600–100, Thermo Fisher Scientific),
589 and 0.02% sodium azide (NaN3, #S2002–25G, Sigma-Aldrich,) in PBS (1 hour at RT).
590 Tissues were then incubated with primary antibodies overnight at 4°C. The primary

591 antibodies used were: Myosin7a (rabbit, 1:1000, 25-6790, Proteus Bioscience), Fzd6
592 (goat, 1:250, AF1526, R&D Systems), Dvl2 (rabbit, 1:250, 12037-1-AP, Proteintech,
593 Rosemont, IL), ZO-1 (mouse IgG1, 1:1000, 33-9100, Thermo Fisher Scientific), Ki67 (rat,
594 1:250, rat, 14-5698-82, Thermo Fisher Scientific), Vangl1 (rabbit, 1:1,000, HPA025235,
595 Sigma-Aldrich), Vangl2 (rabbit, 1:250, 21492-1-AP, Proteintech), and Celsr1 (rabbit,
596 1:3,000, gift from E. Fuchs, Rockefeller University). Following incubation with primary
597 antibodies, samples were washed with PBS three times (15 minutes each) and incubated
598 with the following secondary antibodies: Alexa Fluor 488, 546, and 647 (1:400 for all, A-
599 11055, A-10040, A-31571, Thermo Fisher Scientific) and DAPI (1:10,000, Invitrogen) at
600 room temperature for 2 hours. To label f-actin, phalloidin conjugated with Alexa546 (1:500,
601 A-22283, Thermo Fisher Scientific) was applied during secondary antibody incubation.
602 EdU detection was performed using the 647 Click-IT kit (C10340, Invitrogen). After
603 staining, cochlear epithelium was mounted in ProLong™ Gold Antifade Mountant
604 (P36930, Thermo Fisher Scientific) and coverslipped. Control and experimental samples
605 were always processed and imaged in parallel.
606

607 **Fluorescent RNA *in situ* hybridization**

608 The whole heads of E16.5 or E18.5 mouse embryos were halved and fixed with 4% PFA
609 in PBS for 16 to 24 hours at 4°C, treated with 10, 20, and 30% sucrose in PBS at 4°C (1
610 hour, 1 hour, and overnight, respectively). After that, tissues were embedded in OCT for
611 cryosections (10 μm). RNAScope and BaseScope assays were performed as follows:
612 tissue sections were hybridized with commercial probes from Advanced Cell Diagnostics
613 (ACDbio). These probes were specifically designed to detect deleted regions of the

614 following genes in that were deleted: Wls, Wnt5a, Wnt7a, and Wnt7b. The sections were
615 counterstained with anti-Myosin7a (rabbit, 1:1000, 25-6790, Proteus Bioscience) and
616 Sox2 (goat, 1:200, AF2018, R&D Systems) antibodies. The use of these antibodies was
617 done according to the manufacturer's instructions for fixed frozen sections. DAPI
618 (1:10,000, Invitrogen) was also used for nuclear staining. Briefly, sections were washed
619 in PBS for 5 mins once and then treated with H_2O_2 for 10 minutes. Next, the sections
620 were permeabilized using a target retrieval reagent (ACDbio) and proteinase prior to
621 hybridization. The following probes were used: DapB (Cat No. 310043), Polr2a (Cat No.
622 310451), Wls (Cat No. 405011), Wnt5a-2EJ (Cat No. 717251), Wnt7a-3zz-st-C1 (Cat No.
623 1277921-C1), and Wnt7b-2zz-st-C1 (Cat No. 1275011-C1) (all from Advanced Cell
624 Diagnostics). Control and cKO samples were processed and imaged in parallel.
625

626 **Imaging and quantification**

627 Immunofluorescence or *in situ* hybridization samples were imaged using a Zeiss LSM700
628 or LSM880 confocal microscope in conjunction with Zen software (Zeiss). Image analysis,
629 including measurements of cochlear length and hair cell orientation, was performed using
630 ImageJ software as described below (NIH).

631 Wholemount preparation and cochlear section were used to assess proliferation in
632 the cochlear epithelium and of periotic mesenchymal cells, respectively. For the former,
633 Sox2+ cells in the cochlear epithelium in the basal, middle, and apical regions were used
634 to calculate the percent Edu+ or Ki67+. For the POM, 20-50 DAPI+ cells from three areas
635 (lateral wall, perimodiolar, and basilar membrane) in the basal, middle, and apical regions
636 of the cochlea were used to calculate of the percent of Edu+ or Ki67+ cells. The basal,

637 middle, and apical regions were defined as 25, 50, and 70% length from the basal end of
638 the cochlear epithelium.
639
640 **Hair cell orientation measurement**
641 Whole mount preparation of the basal and middle turns of the right cochlea was used.
642 The orientation of individual hair cells was defined as previously described[15]. Specifically,
643 using ImageJ, a line was drawn parallel to the pillar cells (a reference line), and another
644 line was drawn from the base to the apex of bundles of individual hair cells (a hair bundle
645 line). Then, the angle between the hair bundle and reference lines was used to determine
646 the orientation of the hair cell (in degrees, counterclockwise direction is positive). Thirty
647 to 50 hair cells for each row from one cochlea from each mouse were measured (IHC,
648 OHC1, OHC2, OHC3, and additional rows more lateral to the OHC3 are denoted as
649 OHC3+). Three to six mice for each genotype were examined. Polar coordinate histogram
650 plots depicting hair cell orientation at each row and condition were generated and
651 statistics including the circular mean, mean resultant length, standard deviation, and
652 variance were calculated in using Python and the code is available on GitHub
653 (https://github.com/tahajanlab/published/tree/main/Kishimoto_et_al).
654
655 **Inferred Cell-Cell Communication Analysis**
656 To include both epithelial cells and mesenchymal cells in the cell-cell communication
657 analyses, we merged previously published E14.5/E16.5 epithelial-enriched data (GEO
658 Accession GSE137299[39]) with E13.5/E15.5 mesenchymal-enriched datasets (GEO
659 Accession GSE178931[38]; GEO Accession GSE217727[40]) in Seurat v5.3.0 merge function

660 resulting in combined raw count matrices[78]. The merged data was then log transformed,
661 normalized, and scaled for sequencing depth. Linear dimensionality reduction was then
662 performed via principal component analysis (PCA). For visualization, integration was
663 performed using Harmony[79] and non-linear dimensionality reduction was performed via
664 the uniform manifold approximation and projection (UMAP) algorithm. Cell types were
665 identified by canonical markers for mesenchymal cells (*Pou3f4*), prosensory cells (*Sox2*
666 and *Cdkn1b*), hair cells (*Pou4f3*), and the rest of the epithelial cells (*Epcam*). CellChat
667 was then used to infer cell-cell communication probability based on ligand and receptor
668 gene expression. Normalized count data was imported into CellChat v2.1.2 and the
669 CellChatDB mouse database was used[41]. Communication probability was calculated
670 based on the 10% truncated mean (average expression after discarding 10% from each
671 end of the data) for each ligand and receptor gene. The p-values were Benjamini-
672 Hochberg adjusted, and a cutoff of an adjusted p-value < 0.05 was considered statistically
673 significant. Chord plots were used to visualize directed ligand-receptor interactions for the
674 WNT and non-canonical WNT signaling pathways with a specific focus on hair cells and
675 prosensory cells as signal receivers. Bar graphs were also used to show relative
676 contributions of cell signaling from hair cells, prosensory cells, and epithelial cells.
677

678 **Statistical analysis**

679 For the comparison of cochlear length and hair cell counts, we performed either a two-
680 tailed unpaired Student's t-test, or a one-way ANOVA followed by Tukey's or Šídák's
681 multiple comparisons test. The Ki67- or EdU-positive ratios were evaluated using a two-
682 tailed unpaired Student's t-test. Student’s t-test and ANOVA were conducted using

683 GraphPad Prism version 10 (GraphPad Software), with statistical significance set at $P <$
684 0.05. The N values indicate the number of hair cells in circular histograms and the number
685 of mice in other experiments.
686
687 **Hair cell orientation analysis**
688 The data comprised 11 individual experiment groups, each comparing the angle for hair
689 bundle orientation between control and cKO mice. Measurements were taken in a
690 patterned way for each mouse in each experiment group: from hair cells from four different
691 rows (IHC, OHC1, OHC2, and OHC3 rows) and at two cochlear turns (the basal and
692 middle turns), leading to 8 possible combinations.
693 A Bayesian mixed model analysis was run separately for each conditional KO
694 using the R package bpnreg v2.0.3[80] (Cremers, Jolien. n.d. Bpnreg: Bayesian Projected
695 Normal Regression Models for Circular Data. https://github.com/joliencremers/bpnreg)
696 with fixed effects treatment, i.e. control or conditional KO mice, and for cochlear turn
697 (basal and middle), and hair cells from four different rows (IHC, OHC1, OHC2, and OHC3
698 rows) along with random effects for the individual mice. Due to the limited number of mice
699 (n=6-8), the regression model was either a simple additive model or one containing the
700 interaction between cochlear turn and hair cell row. The bpnreg package respects the
701 circular nature of the angle measurements and yields samples from the posterior
702 distributions for the regression coefficients. Convergence of the underlying Markov Chain
703 was assessed via traceplots. The final model chosen for analysis (additive vs. interaction)
704 was based on Watanabe-Akaike criterion. Posterior samples from the selected model
705 were used to assess the difference in angles for each of the eight cochlear turn and hair

706 cell row combination between conditional KO and control groups. Each difference was
707 judged to be significant based on whether the posterior 95% credible intervals missed the
708 origin or not (Supplementary Table 1). The circular variance ratio was defined as the
709 circular variance of hair cell orientation in the KO group divided by the circular variance
710 of hair cell orientation in the control group.
711

712 **Acknowledgments**

713 We thank our lab members for insightful comments on the manuscript, W. Dong for
714 excellent technical support, E. Fuchs (Rockefeller University) for sharing the Celsr1
715 antibody. The *Wnt7a*$^{flox/flox}$ mice were kindly shared by Jeremy Nathans (Johns Hopkins
716 University), *Emx2*$^{Cre/+}$ mice by Angelika Doetzlhofer (Johns Hopkins University), and
717 *Dermo1(Twist2)*$^{Cre/+}$ mice by Sung-Ho Huh (University of Mississippi). This work was
718 supported by JSPS (Japan Society for the Promotion of Science) Overseas Research
719 Fellowships (IK), NIH (National Institutes of Health) UM1TR004921 (BN), K08DC019683,
720 R21DC022058 (TAJ), NIH/NIDCD Division of Intramural Research fund DC000094-01
721 (RH), R01DC021110, R01DC016919 (AGC), the Stanford Initiative to Cure Hearing Loss.
722 This research was supported in part by the Intramural Research Program of the NIH. The
723 contributions of the NIH authors are considered Works of the United States Government.
724 The findings and conclusions presented in this paper are those of the authors and do not
725 necessarily reflect the views of the NIH or the U.S. Department of Health and Human
726 Services.
727

728 **Author contribution**

729 I.K., E.L.S., W.D., and S.E.B. performed experiments and collected data; A.P.D., K.P.R.,
730 R.H., and T.A.J. performed computational analysis on single-cell data, B.N. and B.E., and
731 A.P.D. performed statistical analysis on hair cell orientation, I.K., S.E.B., and A.G.C.
732 designed experiments; I.K., A.P.D., K.P.R., B.N., and A.G.C. drafted the manuscript.
733

734 **Code Availability**

735 The following publicly available algorithms and software were used for data analysis
736 presented in this manuscript: Seurat (v5.3.0), CellChat (v2.1.2), and R (v4.5.2) package
737 bpnreg (v2.0.3).
738

739 **Figure legend**

740 **Figure 1. Deletion of Wntless shortens the cochlea and causes mild hair cell**
741 **malrotation. a.** Transgenic approach to delete Wntless in the cochlear epithelium. Cre
742 recombinase in the Emx2-Cre cochlear epithelium begins around embryonic day (E) 10.5.
743 **b-c.** Immunostaining and fluorescence *in situ* hybridization showing *Wls* mRNA in the
744 cochlear epithelium in controls ($Emx2^{Cre/+}$; $Wls^{flox/+}$), and no Wls mRNA signals in the
745 cochlear epithelium of $Emx2^{Cre/+}$; $Wls^{flox/flox}$ (Emx2-Wls cKO) mice. **d.** Whole mount
746 preparation of E18.5 cochlea immunostained for Myo7A, showing shortened Emx2-Wls
747 cKO cochlea. **e.** Emx2-Wls cochleae are significantly shorter than controls at E18.5. **f.**
748 There are fewer Myo7A-positive hair cells per cochlea in Emx2-Wls cKO than controls.
749 **g-h.** Hair cells in Emx2-Wls cKO cochlea exhibit more variable orientations compared to
750 controls. **i.** Circular histograms depicting the distribution of hair bundle orientation in the
751 basal turn of control and Emx2-Wls cKO cochleae, with the latter showing significantly

752 larger circular variance and different average orientation in the IHC, OHC1, and OHC3+
753 rows. The OHC3+ row represents the third and more lateral rows of OHCs. **j.** Cartoon
754 illustrating the asymmetric localization of core PCP proteins in hair cells. Dvl2 is present
755 at the lateral pole of HCs, while Fzd6 is at the medial pole. Vangl1 and Vangl2 are present
756 at the lateral side of SCs, and Celsr1 is enriched at the junction between the medial side
757 of HCs and the lateral side of SCs. **k-l.** Immunostaining for Fzd6 and Dvl2, and ZO1 in
758 the basal turn of cochleae from control (k-k’’’) and Emx2-Wls cKO (l-l’’’) mice. Polarized
759 expression of Fzd6 and Dvl2 is observed at the medial and lateral poles of OHCs,
760 respectively, in the control (k’’’, white arrows) but not in the Emx2-Wls cKO cochlea (l’’’,
761 dashed white arrows). **m-p.** Immunostaining showing expression of Vangl2 and Celsr1 in
762 the medial pole of hair cells in control (m, o) and Emx2-Wls cKO cochleae (n, np). Scale
763 bar: 20 μm in (b, c), 200 μm in (d), 5 μm in (g, h), 10 μm in (m-p), 5 μm in (k-k”, l-l”), 2 μm
764 in (k’’’, l’’’). Data are presented as mean ± S.D. and compared using an unpaired t-test. n,
765 number of hair cells measured. Circular mean and variance of hair cell orientation are
766 indicated with blue and red lines in circular histograms, respectively. A Bayesian mixed
767 model analysis used for comparison of circular mean of hair cell orientation between
768 control and cKO groups (see Materials and Methods section for more details).
769 *significantly different (for hair cell orientation analysis), **$p < 0.01$, ****$p < 0.0001$, ns =
770 not significant.
771
772 **Figure 2. Cell-cell communication analysis of the embryonic cochlea. a-b.** UMAP of
773 E13.5 periotic mesenchyme (POM) and E14.5 cochlear epithelium (early embryonic
774 cochlea dataset (a) and of E15.5 POM and E16.5 cochlear epithelium (late embryonic

775 cochlea dataset (b). **c-d.** Circle plot showing an inferred signaling network between Wnt
776 (canonical and non-canonical) ligands and receptors among cell groups from the early (c)
777 and late (d) developing cochlea datasets. The width of arrows is proportional to the
778 probability of communication between any two cell groups and autocrine signaling is
779 represented by a loop. In the early dataset, significant Wnt ligand-receptor interactions
780 are found among the four cell groups. Among the significant interactions, outgoing Wnt
781 ligand signals from hair cells are no longer significant in the late embryonic cochlea
782 dataset. Furthermore, the strength of interactions involving POM is robust in both datasets.
783 **e-f.** Chord plots for cell-cell communication from Wnt ligands and receptors in the early
784 (e) and late (f) developing cochlea datasets, with bands' width reflecting the scale of
785 contribution. **g-j.** Ranked Wnt ligands received by hair cells and prosensory cells in the
786 cochlear epithelium (g, h) or POM (i, j). In the early dataset, Wnt7b is the most potent Wnt
787 ligand emanating from the cochlear epithelium, followed by Wnt7a and Wnt5a (g). In the
788 late dataset, Wnt5a is the most potent Wnt, followed by Wnt7b and Wnt7a (h). Across
789 both datasets, Wnt5a is the most potent among Wnts derived from the POM followed by
790 Wnt5b (i, j). See Source Data file for details.
791
792 **Figure 3. Deletion of multiple Wnts shortens the cochlea and causes mild PCP**
793 **defects**. **a.** Schematic depicting the expression patterns of Wnt5a, Wnt7a, and Wnt7b in
794 the developing mouse cochlear epithelium. **B-C.** Whole mount preparation of E18.5
795 control and *Emx2*$^{Cre/+}$*; Wnt5a*$^{flox/flox}$*; Wnt7a*$^{flox/flox}$*; Wnt7b*$^{flox/flox}$ (Emx2-Wn5a; Wnt7a; Wnt7b
796 cKO) immunostained for Myo7A, with measurements showing that the latter are
797 significantly shorter. **d.** Emx2-Wnt5a; Wnt7a; Wnt7b cKO cochlea had significantly fewer

798 Myo7A-positive hair cells than littermate controls at E18.5. **e**. Measurements of the
799 lengths of cochleae in transgenic mice with deletion of one to multiple Wnts. The length
800 of Emx2-Wn5a; Wnt7a; Wnt7b cKO cochleae was significantly shorter than each of the
801 single or double cKO cochleae, and comparable to that of Emx2-Wls cKO cochleae. **f.**
802 Quantitative analysis of hair cells among control cochleae and cochleae with deletion of
803 one or multiple Wnts. Hair cell counts in Emx2-Wn5a; Wnt7a; Wnt7b cKO cochleae were
804 significantly lower than in each of single or Emx2-Wnt5a; Wnt7a cKO cochleae, and
805 comparable to those in Emx2-Wnt5a; Wnt7b, Emx2-Wnt7a; Wnt7b, or Emx2-Wls cKO
806 cochleae. Hair cell counts in Emx2-Wnt5a; Wnt7b cKO cochleae were significantly lower
807 than Emx2-Wnt5a cKO and Emx2-Wnt7b cKO cochleae ($p < 0.001$ and $p < 0.01$,
808 respectively. **g-h.** Whole mount preparation of E18.5 control (g, g') and Emx2-Wn5a;
809 Wnt7a; Wnt7b cochlea (h, h') immunostained for f-actin. **i.** Circular histograms illustrating
810 the distribution of hair bundle orientations in control and Emx2-Wn5a; Wnt7a; Wnt7b cKO
811 cochleae. No significant misorientation of the hair cells was detected (circular means and
812 variance). **j–k.** Polarized expression of Fzd6 and Dvl2 is observed at the medial and
813 lateral poles of OHCs, respectively, in the basal turn of both control (j''', white arrows) and
814 Emx2-Wn5a; Wnt7a; Wnt7b cKO cochleae (k''', white arrows). Scale bar: 200 μm in (b),
815 5 μm in (g-h, j-j'', k-k''), 2 μm in (j''', k'''). Data are presented as mean ± S.D. and analyzed
816 using an unpaired t-test (c, d) or one-way ANOVA followed by either Šídák's multiple
817 comparisons test (e-f). n, number of hair cells measured. Mean and S.D. of hair cell
818 orientation are indicated with blue and red lines in circular histograms, respectively. A
819 Bayesian mixed model analysis used for comparison of circular mean of hair cell

820 orientation between control and cKO groups. *p < 0.05, **p < 0.01, ***p < 0.001, ****p <
821 0.0001, ns = not significant.
822
823 **Figure 4. Wnt5a deletion from the periotic mesenchyme does not induce cochlear**
824 **PCP defects. a.** Transgenic approach to delete Wnt5a in the POM. Cre recombinase in
825 the POM of Dermo1-Cre cochlea begins around embryonic day (E) 9.5. **d.** Whole mount
826 preparation of cochleae from E18.5 control and Dermo1-Wnt5a cKO embryos. **e-f.**
827 Cochlear lengths and hair cell counts are comparable between control and Dermo1-
828 Wnt5a cKO mice at E18.5. **g-h.** F-actin-stained cochleae from control (g) and Dermo1-
829 Wnt5a cKO (h) embryos at E18.5. **i** Circular histograms demonstrating comparable hair
830 bundle orientation in the basal turn of control and Dermo1-Wnt5a cKO cochleae. **j–j’’’, k–**
831 **k’’’.** Polarized expression of Fzd6 and Dvl2 (white arrows) is observed at the medial and
832 lateral poles of OHCs, respectively, both in the control (j’’’) and the Dermo1-Wnt5a cKO
833 cochlea (k’’’).These results suggest that deletion of Wnt5a alone from the POM does not
834 disrupt cochlear PCP. CD cochlear duct; ST scala tympani; SV scala vestibule; SG spiral
835 ganglion. Scale bar: 20 μm in (b-c’), 5 μm in (g-h, j-k’’’), 200 μm in (d). n, number of hair
836 cells measured. Mean and S.D. of hair cell orientation are indicated with blue and red
837 lines in circular histograms, respectively. A Bayesian mixed model analysis used for
838 comparison of circular mean of hair cell orientation between control and cKO groups. ns
839 = not significant.
840
841 **Figure 5. Deletion of Wntless in the cochlear epithelium and periotic mesenchyme**
842 **causes severe cochlear shortening and PCP defects. a.** Schematic of deleting

843 Wntless using the Sox9-CreERT2; Wntless-flox mice. Tamoxifen (0.2 mg/g) was
844 administered at E10.5 and E11.5 and cochleae were analyzed at E18.5. **b-c.**
845 Immunostaining and measurements of E18.5 control (*Sox9*$^{CreERT2/+}$*; Wls*$^{flox/+}$) and
846 *Sox9*$^{CreERT2/+}$*; Wls*$^{flox/flox}$ (Sox9-Wls cKO) cochleae, showing dramatic shortening of the
847 latter and significantly shorter than both control and Emx2-Wls cKO cochleae. **d.** Sox9-
848 Wls cKO cochleae had significantly fewer cells compared to control and Emx2-Wls cKO
849 cochleae. **e-f.** Whole mount preparation of basal turn of the E18.5 f-actin-stained cochlea
850 The Sox9-Wls cKO cochlea shows five to six rows of hair cells that are disorganized and
851 lack a separation between IHCs and OHCs. Notably, hair cells are mostly malrotated
852 toward the apex. **g** Circular histograms illustrating the distribution of hair bundle
853 orientation in control and Sox9-Wls cKO cochleae, which showed significantly larger
854 circular variance and different average orientation in each row relative to controls. **h-q.**
855 Immunostaining for core PCP proteins in the control and Sox9-Wls cKO cochleae for
856 Celsr1 (h, i), Vangl1 (j, k), Vangl2 (l, m), Fzd6 (n, o), and Dvl2 (p, q), showing a loss of
857 polarized expression of Celsr1, Vangl1, Vangl2, Fzd6, and Dvl2 in OHCs of Sox9-Wls
858 cKO cochleae. **r-s.** Sections of E15.5 control (r) and Sox9-Wls cKO (s) cochleae
859 illustrating Ki67- and EdU-positive cells in both the cochlear epithelium and periotic
860 mesenchyme. **t-u.** Quantitative assessment showing comparable proliferation in the
861 cochlear epithelium between the control and Sox9-Wls cKO cochleae. CD, cochlear duct;
862 LW, POM near the lateral wall; BM, POM near the basilar membrane; PM, perimodiolar
863 POM. Scale bar: 200 μm in (b), 5 μm in (e-f, h-q), 40 μm in (r-s). Data are presented as
864 mean ± S.D. and analyzed using one-way ANOVA followed by Tukey's multiple
865 comparisons test (c-d) and an unpaired t-test (t-u). n, number of hair cells measured.

866 Mean and S.D. of hair cell orientation are indicated with blue and red lines in circular
867 histograms, respectively. A Bayesian mixed model analysis used for comparison of
868 circular mean of hair cell orientation between control and cKO groups. *significantly
869 different (for hair cell orientation analysis), **$p < 0.01$, ****$p < 0.0001$, ns = not significant.
870
871 **Figure 6. Working model of epithelial and mesenchymal Wnts coordinating to**
872 **regulate cochlear elongation, hair cell orientation, and PCP signaling.** When only
873 mesenchymal Wnts are present, cochlear length is mildly shortened and hair cells mildly
874 misoriented and most core PCP proteins are present. In the absence of both epithelial
875 and mesenchymal Wnts, cochlear duct is severely shortened, and hair cells severely
876 malrotated toward the apex.
877
878 **Supplementary Figure 1. In situ hybridization and hair bundle orientation in the**
879 **Emx2-Wls cKO cochlea. a-b.** Negative (DapB) and positive (Polr2a) controls for *in situ*
880 hybridization in E16.5 cochleae. **c-h.** RNA scope *in situ* hybridization of Wls mRNA in the
881 basal, middle, and apical turn of the control (c-c'', e-e'', g-g'') and Emx2-Wls cKO (d-d'', f-
882 f'', h-h'') cochleae. Magnified views (white boxes) of the cochlear epithelium and POM are
883 shown in (c'-h') and (c''-h''), respectively. In Emx2-Wls cKO cochleae, Wls mRNA is
884 almost undetectable in the cochlear epithelium, while that in the POM remain comparable
885 to those in control cochleae. **i-j.** Whole mount preparation of the Emx2-Wls cKO and
886 control cochlea stained for f-actin. In the Emx2-Wls cKO cochlea, hair cells exhibit more
887 variable orientations compared to controls. **k.** Circular histograms depicting the
888 distribution of hair bundle orientation both control and Emx2-Wls cKO cochleae, showing

889 significantly large variance and the average rotation for the IHC, OHC1, and OHC3 rows
890 in the Emx2-Wls cKO cochleae. CD, cochlear duct; ST, scala tympani; SV, scala vestibule;
891 SG, spiral ganglion. Scale bar: 20 μm in (a-h''), 5 μm in (I, j). n, number of hair cells
892 measured. Circular mean and variance of hair cell orientation are indicated with blue and
893 red lines in circular histograms, respectively. A Bayesian mixed model analysis used for
894 comparison of circular mean of hair cell orientation between control and cKO groups.
895 *significantly different (for hair cell orientation analysis), ns = not significant.
896
897 **Supplementary Figure 2. Expression of Wnt5a, Wnt7a, and Wnt7b mRNA in the**
898 **control and conditional knockout cochlea. a-d.** *Wnt5a* mRNA is robustly expressed in
899 the epithelium and periotic mesenchyme of control cochlea (a, c) and is almost
900 undetectable in the epithelium of Emx2-Wnt5a cKO (b, d) cochleae. **e-h.** Wnt7a mRNA is
901 robustly expressed in the epithelium of the control cochlea (e, g) and is barely detectable
902 in the Emx2-Wnt7a cKO (f, h) cochleae. **i-l.** Wnt7b mRNA is robustly expressed in the
903 epithelium of the control cochlear (I, k) and is almost undetectable in the Emx2-Wnt7b
904 cKO (j, l) cochleae. Scale bar: 20 μm.
905
906 **Supplementary Figure 3. Cochlear length and core PCP protein expression in**
907 **Wnt5a, Wnt7a, and Wnt7b cKO cochlea. a-b, f-g, k-m.** Comparable lengths between
908 Myo7a-marked controls and cochleae from Emx2-Wnt5a (a), Emx2-Wnt7a (f), and Emx2-
909 Wnt7b cKO (k) mice at E18.5. **c, h, m** Hair cell counts show no significant differences
910 between Emx2-Wnt5a (b) and Emx2-Wnt7a cKO (g) mice and their littermate controls,
911 whereas those from Emx2-Wnt7b cKO (l) mice are slightly reduced compared to controls

912 at E18.5. **d-e’’’, i-j’’’, n-o’’’** Polarized expression of Fzd6 and Dvl2 (white arrows) at the
913 medial and lateral poles of OHCs, respectively, in control cochleae and cKO cochleae for
914 Wnt5a (d’’’ and e’’’,), Wnt7a (i’’’ and j’’’), and Wnt7b (n’’’ and o’’’). Data are presented as
915 mean ± S.D. and compared using an unpaired t-test. Scale bars: 200 μm in (a, f, k); 5 μm
916 in (d-d’’, e-e’’, i-i”, j-j’’, n-n”, o-o”); 2 μm in (d’’’, e’’’, i’’’, j’’’, n’’’, o’’’). Data are presented as
917 mean ± S.D. and compared using an unpaired t-test. *p < 0.05, ns = not significant.
918
919 **Supplementary Figure 4. Hair bundle orientation of the cochlea from Emx2-Wnt5a,**
920 **Emx2-Wnt7a, and Emx2-Wnt7b cKO mice. a-d, g-j, m-p.** F-actin-stained cochleae from
921 Emx2-Wnt5a (a-d), Emx2-Wnt7a (g-j), and Emx2-Wnt7b cKO (m-p) mice at E18.5. **e, f,**
922 **k, l, q, r.** Circular histograms demonstrating no significant variance or average deviation
923 hair bundle orientation in Emx2-Wnt5a (e, f) and Emx2-Wnt7a (k, l) cKO cochleae. and
924 For Emx2-Wnt7b cKO (q, r) cochlea, there was no significant variance, but significantly
925 different circular means of hair cell orientation compared to controls was detected for the
926 IHC, OHC1, and OHC2 rows. Scale bar: 5 μm. n, number of hair cells measured. Circular
927 mean and variance of hair cell orientation are indicated with blue and red lines in circular
928 histograms, respectively. A Bayesian mixed model analysis used for comparison of
929 circular mean of hair cell orientation between control and cKO groups. *significantly
930 different (for hair cell orientation analysis), ns = not significant.
931
932 **Supplementary Figure 5. Cochlear length and core PCP protein expression after**
933 **deletion of Wnts. a-b, f-g, k-l.** Whole mount preparation of cochleae from Emx2-Wnt5a;
934 Wnt7a (a-b), Emx2-Wnt5a; Wnt7b (f-g), and Emx2-Wnt7a; Wnt7b cKO (k-l) mice and their

935 littermate controls at E18.5. The lengths of Emx2-Wnt5a; Wnt7b and Emx2-Wnt7a; Wnt7b
936 cKO, but not Emx2-Wnt5a; Wnt7a cKO, cochleae were significantly shorter than those of
937 controls. **c, h, m** Hair cell counts show no significant differences between Emx2-Wnt5a;
938 Wnt7a (c) and Emx2-Wnt7a; Wnt7b cKO (m) cochleae and their littermate controls,
939 whereas those from Emx2-Wnt5a; Wnt7b cKO (h) cochleae are slightly reduced
940 compared to controls at E18.5. **d-e''', i-j''', n-o'''** Polarized expression of Fzd6 and Dvl2
941 is observed at the medial and lateral poles of OHCs, respectively, in control cochlea and
942 cKO cochleae for Wnt5a and Wnt7a (d''' and e''', white arrows), Wnt5a and Wnt7b (i''' and
943 j''', white arrows), and Wnt7a and Wnt7b (n''' and o''', white arrows). Data are presented
944 as mean ± S.D. and compared using an unpaired t-test. Scale bars: 200 μm in (a, f, k);
945 5 μm in (d-d'', e-e'', i-i'', j-j'', n-n'', o-o''); 2 μm in (d''', e''', i''', j''', n''', o'''). **p < 0.01, ***p <
946 0.001, ****p < 0.0001, ns = not significant.
947
948 **Supplementary Figure 6. Hair bundle orientation after deletion of Wnt members the**
949 **cochlear epithelium. a-d, g-j, m-p.** F-actin-stained cochleae from Emx2-Wnt5a; Wnt7a
950 (a-d), Emx2-Wnt5a; Wnt7b (g-j), and Emx2-Wnt7a; Wnt7b cKO (m-p) mice at E18.5. **e, f,**
951 **k, l, q, r.** Circular histograms demonstrating the distribution of hair bundle orientation in
952 the cochlea from Emx2-Wnt5a; Wnt7a (e, f), Emx2-Wnt5a; Wnt7b (k, l), and Emx2-Wnt7a;
953 Wnt7b cKO (q, r) mice at E18.5. Emx2-Wnt5a; Wnt7a cKO cochleae show normal hair
954 cell orientation. Emx2-Wnt5a; Wnt7b cKO cochleae exhibit more variable orientations of
955 hair cells compared to controls (g-j), confirmed by significantly larger circular variance in
956 hair cell orientation, but the average orientation was not significantly different from
957 controls, with the exception of the IHC row of the basal turn. Similarly, hair cell variance

958 in Emx2-Wnt7a; Wnt7b cKO cochleae was not significantly different from controls, with
959 no significantly different circular mean except for the OHC3 row. Scale bar: 5 μm. n,
960 number of hair cells measured. Circular mean and variance of hair cell orientation are
961 indicated with blue and red lines in circular histograms, respectively. A Bayesian mixed
962 model analysis used for comparison of circular mean of hair cell orientation between
963 control and cKO groups. *significantly different, ns = not significant.
964
965 **Supplementary Figure 7. Hair bundle orientation after deletion of three Wnt**
966 **members in the cochlear epithelium.** Whole mount preparation of f-actin-stained
967 cochlea from control (a, a') and Emx2-Wn5a; Wnt7a; Wnt7b cKO (b, b') mice. **i** Circular
968 histograms illustrating the distribution of hair bundle orientations in the middle turn of both
969 control and Emx2-Wn5a; Wnt7a; Wnt7b cKO cochleae, showing no significant difference
970 in circular means and variance from controls. n, number of hair cells measured. Circular
971 mean and variance of hair cell orientation are indicated with blue and red lines in circular
972 histograms, respectively. A Bayesian mixed model analysis used for comparison of
973 circular mean of hair cell orientation between control and cKO groups. ns = not significant.
974
975 **Supplementary Figure 8. In situ hybridization of Wnt5a mRNA in the Dermo1-Wnt5a**
976 **cKO cochlea.** Wnt5a mRNA is robustly expressed in the cochlear duct and periotic
977 mesenchyme of the control cochleae (*Dermo1*$^{Cre/+}$; *Wnt5a*$^{flox/+}$) (a-a', c-c'), and notably
978 absent in the periotic mesenchyme of *Dermo1*$^{Cre/+}$; *Wnt5a*$^{flox/flox}$ cochleae (Dermo1-
979 Wnt5a) (b-b', d-d') at E16.5. Wnt5a mRNA remain present in the cochlear epithelium and
980 spiral ganglion (b-b', d-d'), indicating effective deletion of Wnt5a mRNA specifically from

981 the POM. **e-g.** F-actin-stained middle turn of cochleae from control (e) and Dermo1-
982 Wnt5a cKO (f) embryos at E18.5. **i** Circular histograms demonstrating comparable hair
983 bundle orientation in the middle turn of control and Dermo1-Wnt5a cKO cochleae. CD
984 cochlear duct; ST scala tympani; SV scala vestibule; SG spiral ganglion. Scale bar: 20 μm
985 in (a-h''), 5 μm in (I, j). A Bayesian mixed model analysis used for comparison of circular
986 mean of hair cell orientation between control and cKO groups. ns = not significant.
987
988 **Supplementary Figure 9. Deleting Wntless in the cochlear epithelium and periotic**
989 **mesenchyme at E11.5/12.5 causes mild PCP defects. a.** Schematic of broadly deleting
990 Wntless using the Sox9-CreERT2; Wntless-flox mice. Tamoxifen (0.2 mg/g) was
991 administered at E11.5 and E12.5 and cochleae were analyzed at E18.5. **b.** Sox9-Wls cKO
992 cochlea is significantly shorter than controls. **c-d.** Length and hair cell counts of Sox9-Wls
993 cKO cochleae with tamoxifen administered at E11.5-12.5 were significantly lower than
994 controls, but higher than Sox9-Wls cKO cochleae with tamoxifen administered at E10.5-
995 11.5. **e-h.** Whole mount preparation of f-actin-stained cochlea showing hair cells
996 malrotated towards the apex in the Sox9-Wls cKO cochlea (arrows). **i-j.** Circular
997 histograms demonstrating the distribution of hair bundle orientation in control and Sox9-
998 Wls cKO cochleae. Significantly larger circular variance and different circular means of
999 hair cell orientation are detected in the basal and middle turns of Sox9-Wls cKO cochleae.
1000 **k-s.** Control and Sox9-Wls cKO cochleae showed polarized expression of core PCP
1001 proteins in (Fzd6 (k-l), Celsr1 (m-n), Vangl1 (p-q), and Vangl2 (r-s)). Scale bar: 200 μm
1002 in (b), 5 μm in (e-h, k-s). Data are presented as mean ± S.D. and analyzed using one-way
1003 ANOVA followed by Tukey's multiple comparisons test. n, number of hair cells measured.

1004 Circular mean and variance of hair cell orientation are indicated with blue and red lines in
1005 circular histograms, respectively. A Bayesian mixed model analysis used for comparison
1006 of circular mean of hair cell orientation between control and cKO groups. *significantly
1007 different (for hair cell orientation analysis), **$p < 0.01$, ***$p < 0.001$, ****$p < 0.0001$, ns =
1008 not significant.
1009
1010 **Supplementary Figure 10. Loss of Wls mRNA expression in Sox9-Wls cKO**
1011 **cochleae. a-f'** In situ hybridization showing robust Wls mRNA expression in all turns of
1012 control (a-a', c-c', e-e') cochleae, and loss of expression in Sox9-Wls cKO (b-b', d-d', f-f')
1013 cochleae at E18.5. Scale bar: 50 μm. CD cochlear duct; ST scala tympani; SV scala
1014 vestibule; SG spiral ganglion.
1015
1016 **Supplementary Figure 11. Hair bundle orientation and proliferation in Sox9-Wls**
1017 **cochlea after Wntless at E10.5 and E11.5. a-b'.** F-actin-stained cochlea from Sox9-Wls
1018 cKO (b, b') embryos showing five to six rows of hair cells, disorganized hair cells lacking
1019 a clear separation between IHCs and OHCs, and malrotation of hair cells toward the apex.
1020 **c.** Circular histograms illustrating the distribution of hair bundle orientation in IHCs and
1021 OHCs in the middle turn of control and Sox9-Wls cKO cochleae. Sox9-Wls cKO cochleae
1022 have significantly larger circular variance for combined IHC and OHCs and significantly
1023 different circular means of hair cell orientation for each of IHC and OHC rows compared
1024 to controls. **d-e.** Whole-mount preparation of E15.5 cochlea labeled with EdU or
1025 immunostained for Ki67, showing comparable degree of proliferation of Sox2-positive
1026 cells in control and Sox9-Wls cKO organs. **f-g.** Proliferation of POM cells in the POM was

1027 not significantly different between control and Sox9-Wls cKO cochleae at E15.5. Data are
1028 presented as mean ± S.D. and analyzed using an unpaired t-test (d-e). n, number of hair
1029 cells measured. Circular mean and variance of hair cell orientation are indicated with blue
1030 and red lines in circular histograms, respectively. A Bayesian mixed model analysis used
1031 for comparison of circular mean of hair cell orientation between control and cKO groups.
1032 *significantly different (for hair cell orientation analysis), ns = not significant.
1033

1034 **References**

1035 1. Cantos R, Cole LK, Acampora D, Simeone A, Wu DK. Patterning of the mammalian
1036 cochlea. *Proc Natl Acad Sci U S A* **97**, 11707-11713 (2000).

1037 2. Driver EC, Kelley MW. Development of the cochlea. *Development* **147**, (2020).

1038 3. Ruben RJ. Development of the inner ear of the mouse: a radioautographic study
1039 of terminal mitoses. *Acta Otolaryngol*, Suppl 220:221-244 (1967).

1040 4. Chen P, Segil N. p27(Kip1) links cell proliferation to morphogenesis in the
1041 developing organ of Corti. *Development* **126**, 1581-1590 (1999).

1042 5. Tarchini B, Lu X. New insights into regulation and function of planar polarity in the
1043 inner ear. *Neurosci Lett* **709**, 134373 (2019).

1044 6. Kelly M, Chen P. Shaping the mammalian auditory sensory organ by the planar
1045 cell polarity pathway. *Int J Dev Biol* **51**, 535-547 (2007).

1046 7. Ross AJ*, et al.* Disruption of Bardet-Biedl syndrome ciliary proteins perturbs planar
1047 cell polarity in vertebrates. *Nat Genet* **37**, 1135-1140 (2005).

1048 8. Jagger D*, et al.* Alstrom Syndrome protein ALMS1 localizes to basal bodies of
1049 cochlear hair cells and regulates cilium-dependent planar cell polarity. *Hum Mol*
1050 *Genet* **20**, 466-481 (2011).

1051 9. Marshall JD, Maffei P, Collin GB, Naggert JK. Alstrom syndrome: genetics and
1052 clinical overview. *Curr Genomics* **12**, 225-235 (2011).

1053 10. Montcouquiol M, Rachel RA, Lanford PJ, Copeland NG, Jenkins NA, Kelley MW.
1054 Identification of Vangl2 and Scrb1 as planar polarity genes in mammals. *Nature*
1055 **423**, 173-177 (2003).

1056 11. Montcouquiol M*, et al.* Asymmetric localization of Vangl2 and Fz3 indicate novel
1057 mechanisms for planar cell polarity in mammals. *J Neurosci* **26**, 5265-5275 (2006).

1058 12. Wang Y, Guo N, Nathans J. The role of Frizzled3 and Frizzled6 in neural tube
1059 closure and in the planar polarity of inner-ear sensory hair cells. *J Neurosci* **26**,
1060 2147-2156 (2006).

1061 13. Etheridge SL*, et al.* Murine dishevelled 3 functions in redundant pathways with
1062 dishevelled 1 and 2 in normal cardiac outflow tract, cochlea, and neural tube
1063 development. *PLoS genetics* **4**, e1000259 (2008).

1064 14. Wang J*, et al.* Regulation of polarized extension and planar cell polarity in the
1065 cochlea by the vertebrate PCP pathway. *Nat Genet* **37**, 980-985 (2005).

1066 15. Najarro EH, Huang J, Jacobo A, Quiruz LA, Grillet N, Cheng AG. Dual regulation
1067 of planar polarization by secreted Wnts and Vangl2 in the developing mouse
1068 cochlea. *Development* **147**, (2020).

1069 16. Torban E*, et al.* Genetic interaction between members of the Vangl family causes
1070 neural tube defects in mice. *Proc Natl Acad Sci U S A* **105**, 3449-3454 (2008).

1071 17. Curtin JA*, et al.* Mutation of Celsr1 disrupts planar polarity of inner ear hair cells
1072 and causes severe neural tube defects in the mouse. *Curr Biol* **13**, 1129-1133
1073 (2003).

1074 18. Steinhart Z, Angers S. Wnt signaling in development and tissue homeostasis.
1075 *Development* **145**, (2018).

1076 19. Xue C, Chu Q, Shi Q, Zeng Y, Lu J, Li L. Wnt signaling pathways in biology and
1077 disease: mechanisms and therapeutic advances. *Signal Transduct Target Ther* **10**,
1078 106 (2025).

1079 20. van Amerongen R. Alternative Wnt pathways and receptors. *Cold Spring Harb*
1080 *Perspect Biol* **4**, (2012).

1081 21. Shi F, Hu L, Jacques BE, Mulvaney JF, Dabdoub A, Edge AS. beta-Catenin is
1082 required for hair-cell differentiation in the cochlea. *J Neurosci* **34**, 6470-6479
1083 (2014).

1084 22. Jansson L*, et al.* beta-Catenin is required for radial cell patterning and identity in
1085 the developing mouse cochlea. *Proc Natl Acad Sci U S A* **116**, 21054-21060 (2019).

1086 23. Ebeid M, Kishimoto I, Roy P, Zaidi MAA, Cheng AG, Huh SH. beta-Catenin
1087 transcriptional activity is required for establishment of inner pillar cell identity during
1088 cochlear development. *PLoS Genet* **19**, e1010925 (2023).

1089 24. Gao B. Wnt regulation of planar cell polarity (PCP). *Curr Top Dev Biol* **101**, 263-
1090 295 (2012).

1091 25. Butler MT, Wallingford JB. Planar cell polarity in development and disease. *Nat*
1092 *Rev Mol Cell Biol* **18**, 375-388 (2017).

1093 26. Munnamalai V, Fekete DM. Notch-Wnt-Bmp crosstalk regulates radial patterning
1094 in the mouse cochlea in a spatiotemporal manner. *Development* **143**, 4003-4015
1095 (2016).

1096 27. Noda T, Oki S, Kitajima K, Harada T, Komune S, Meno C. Restriction of Wnt
1097 signaling in the dorsal otocyst determines semicircular canal formation in the
1098 mouse embryo. *Dev Biol* **362**, 83-93 (2012).

1099 28. Dabdoub A*, et al.* Wnt signaling mediates reorientation of outer hair cell
1100 stereociliary bundles in the mammalian cochlea. *Development* **130**, 2375-2384
1101 (2003).

1102 29. Qian D*, et al.* Wnt5a functions in planar cell polarity regulation in mice. *Dev Biol*
1103 **306**, 121-133 (2007).

1104 30. Xie N*, et al.* Wnt7b acts in concert with Wnt5a to regulate tissue elongation and
1105 planar cell polarity via noncanonical Wnt signaling. *Proc Natl Acad Sci U S A* **121**,
1106 e2405217121 (2024).

1107 31. Landin Malt A, Hogan AK, Smith CD, Madani MS, Lu X. Wnts regulate planar cell
1108 polarity via heterotrimeric G protein and PI3K signaling. *J Cell Biol* **219**, (2020).

1109 32. Deans MR. Conserved and Divergent Principles of Planar Polarity Revealed by
1110 Hair Cell Development and Function. *Front Neurosci* **15**, 742391 (2021).

1111 33. Kindt KS, Tarchini B. Not a hair out of place: Polarizing and orienting sensory hair
1112 cells. *Curr Top Dev Biol* **165**, 85-124 (2025).

1113 34. Banziger C, Soldini D, Schutt C, Zipperlen P, Hausmann G, Basler K. Wntless, a
1114 conserved membrane protein dedicated to the secretion of Wnt proteins from
1115 signaling cells. *Cell* **125**, 509-522 (2006).

1116 35. Wolf L, Boutros M. The role of Evi/Wntless in exporting Wnt proteins. *Development*
1117 **150**, (2023).

1118 36. Ono K*, et al.* FGFR1-Frs2/3 signalling maintains sensory progenitors during inner
1119 ear hair cell formation. *PLoS Genet* **10**, e1004118 (2014).

1120 37. Copley CO, Duncan JS, Liu C, Cheng H, Deans MR. Postnatal refinement of
1121 auditory hair cell planar polarity deficits occurs in the absence of Vangl2. *J*
1122 *Neurosci* **33**, 14001-14016 (2013).

1123 38. Sun Y*, et al.* Single-cell transcriptomic landscapes of the otic neuronal lineage at
1124 multiple early embryonic ages. *Cell Rep* **38**, 110542 (2022).

1125 39. Kolla L*, et al.* Characterization of the development of the mouse cochlear
1126 epithelium at the single cell level. *Nat Commun* **11**, 2389 (2020).

1127 40. Rose KP*, et al.* Spatially distinct otic mesenchyme cells show molecular and
1128 functional heterogeneity patterns before hearing onset. *iScience* **26**, 107769
1129 (2023).

1130 41. Jin S*, et al.* Inference and analysis of cell-cell communication using CellChat. *Nat*
1131 *Commun* **12**, 1088 (2021).

1132 42. Ryu YK, Collins SE, Ho HY, Zhao H, Kuruvilla R. An autocrine Wnt5a-Ror signaling
1133 loop mediates sympathetic target innervation. *Dev Biol* **377**, 79-89 (2013).

1134 43. Dunlap KA*, et al.* Postnatal deletion of Wnt7a inhibits uterine gland morphogenesis
1135 and compromises adult fertility in mice. *Biol Reprod* **85**, 386-396 (2011).

1136 44. Rajagopal J*, et al.* Wnt7b stimulates embryonic lung growth by coordinately
1137 increasing the replication of epithelium and mesenchyme. *Development* **135**,
1138 1625-1634 (2008).

1139

1140 45. Riccomagno MM, Takada S, Epstein DJ. Wnt-dependent regulation of inner ear
1141 morphogenesis is balanced by the opposing and supporting roles of Shh. *Genes*
1142 *Dev* **19**, 1612-1623 (2005).

1143 46. Liu W, Li L, Li G, Garritano F, Shanske A, Frenz DA. Coordinated molecular control
1144 of otic capsule differentiation: functional role of Wnt5a signaling and opposition by
1145 sfrp3 activity. *Growth Factors* **26**, 343-354 (2008).

1146 47. Sosic D, Richardson JA, Yu K, Ornitz DM, Olson EN. Twist regulates cytokine gene
1147 expression through a negative feedback loop that represses NF-kappaB activity.
1148 *Cell* **112**, 169-180 (2003).

1149 48. Huh SH, Warchol ME, Ornitz DM. Cochlear progenitor number is controlled
1150 through mesenchymal FGF receptor signaling. *Elife* **4**, (2015).

1151 49. Cornett B, Snowball J, Varisco BM, Lang R, Whitsett J, Sinner D. Wntless is
1152 required for peripheral lung differentiation and pulmonary vascular development.
1153 *Dev Biol* **379**, 38-52 (2013).

1154 50. Mak AC, Szeto IY, Fritzsch B, Cheah KS. Differential and overlapping expression
1155 pattern of SOX2 and SOX9 in inner ear development. *Gene Expr Patterns* **9**, 444-
1156 453 (2009).

1157 51. Veithen M*, et al.* Sox9 Inhibits Cochlear Hair Cell Fate by Upregulating Hey1 and
1158 HeyL Antagonists of Atoh1. *Cells* **12**, (2023).

1159 52. Sun MR, Steward AC, Sweet EA, Martin AA, Lipinski RJ. Developmental
1160 malformations resulting from high-dose maternal tamoxifen exposure in the mouse.
1161 *PLoS One* **16**, e0256299 (2021).

1162 53. Ved N, Curran A, Ashcroft FM, Sparrow DB. Tamoxifen administration in pregnant
1163 mice can be deleterious to both mother and embryo. *Lab Anim* **53**, 630-633 (2019).

1164 54. Montcouquiol M, Kelley MW. Development and Patterning of the Cochlea: From
1165 Convergent Extension to Planar Polarity. *Cold Spring Harb Perspect Med* **10**,
1166 (2020).

1167 55. Sutherland A, Keller R, Lesko A. Convergent extension in mammalian
1168 morphogenesis. *Semin Cell Dev Biol* **100**, 199-211 (2020).

1169 56. Wu J, Roman AC, Carvajal-Gonzalez JM, Mlodzik M. Wg and Wnt4 provide long-
1170 range directional input to planar cell polarity orientation in Drosophila. *Nat Cell Biol*
1171 **15**, 1045-1055 (2013).

1172 57. Ewen-Campen B, Comyn T, Vogt E, Perrimon N. No Evidence that Wnt Ligands
1173 Are Required for Planar Cell Polarity in Drosophila. *Cell Rep* **32**, 108121 (2020).

1174 58. Yu JJS*, et al.* Frizzled-Dependent Planar Cell Polarity without Secreted Wnt
1175 Ligands. *Dev Cell* **54**, 583-592 e585 (2020).

1176 59. Gros J, Serralbo O, Marcelle C. WNT11 acts as a directional cue to organize the
1177 elongation of early muscle fibres. *Nature* **457**, 589-593 (2009).

1178 60. Gao B*, et al.* Wnt signaling gradients establish planar cell polarity by inducing
1179 Vangl2 phosphorylation through Ror2. *Dev Cell* **20**, 163-176 (2011).

1180 61. Gao B*, et al.* Coordinated directional outgrowth and pattern formation by
1181 integration of Wnt5a and Fgf signaling in planar cell polarity. *Development* **145**,
1182 (2018).

1183 62. Minegishi K*, et al.* A Wnt5 Activity Asymmetry and Intercellular Signaling via PCP
1184 Proteins Polarize Node Cells for Left-Right Symmetry Breaking. *Dev Cell* **40**, 439-
1185 452 e434 (2017).

1186 63. Yang W*, et al.* Wnt-induced Vangl2 phosphorylation is dose-dependently required
1187 for planar cell polarity in mammalian development. *Cell Res* **27**, 1466-1484 (2017).

1188 64. Sienknecht UJ, Anderson BK, Parodi RM, Fantetti KN, Fekete DM. Non-cell-
1189 autonomous planar cell polarity propagation in the auditory sensory epithelium of
1190 vertebrates. *Dev Biol* **352**, 27-39 (2011).

1191 65. Aman A, Piotrowski T. Wnt/beta-catenin and Fgf signaling control collective cell
1192 migration by restricting chemokine receptor expression. *Dev Cell* **15**, 749-761
1193 (2008).

1194 66. Cohen R*, et al.* Mechanical forces drive ordered patterning of hair cells in the
1195 mammalian inner ear. *Nat Commun* **11**, 5137 (2020).

1196 67. Carroll TJ, Park JS, Hayashi S, Majumdar A, McMahon AP. Wnt9b plays a central
1197 role in the regulation of mesenchymal to epithelial transitions underlying
1198 organogenesis of the mammalian urogenital system. *Dev Cell* **9**, 283-292 (2005).

1199 68. Shoshkes-Carmel M*, et al.* Subepithelial telocytes are an important source of Wnts
1200 that supports intestinal crypts. *Nature* **557**, 242-246 (2018).

1201 69. Aros CJ*, et al.* Distinct Spatiotemporally Dynamic Wnt-Secreting Niches Regulate
1202 Proximal Airway Regeneration and Aging. *Cell Stem Cell* **27**, 413-429 e414 (2020).

1203 70. Maimets M*, et al.* Mesenchymal-epithelial crosstalk shapes intestinal
1204 regionalisation via Wnt and Shh signalling. *Nat Commun* **13**, 715 (2022).

1205 71. Stewart RA, Ramakrishnan AB, Cadigan KM. Diffusion and function of Wnt ligands.
1206 *PLoS Genet* **15**, e1008154 (2019).

1207 72. Mii Y*, et al.* Quantitative analyses reveal extracellular dynamics of Wnt ligands in
1208 Xenopus embryos. *Elife* **10**, (2021).

1209 73. Farin HF*, et al.* Visualization of a short-range Wnt gradient in the intestinal stem-
1210 cell niche. *Nature* **530**, 340-343 (2016).

1211 74. Jansson L, Kim GS, Cheng AG. Making sense of Wnt signaling-linking hair cell
1212 regeneration to development. *Front Cell Neurosci* **9**, 66 (2015).

1213 75. Carpenter AC, Rao S, Wells JM, Campbell K, Lang RA. Generation of mice with a
1214 conditional null allele for Wntless. *Genesis* **48**, 554-558 (2010).

1215 76. Kopp JL*, et al.* Sox9+ ductal cells are multipotent progenitors throughout
1216 development but do not produce new endocrine cells in the normal or injured adult
1217 pancreas. *Development* **138**, 653-665 (2011).

1218 77. Yu K*, et al.* Conditional inactivation of FGF receptor 2 reveals an essential role for
1219 FGF signaling in the regulation of osteoblast function and bone growth.
1220 *Development* **130**, 3063-3074 (2003).

1221 78. Hao Y*, et al.* Dictionary learning for integrative, multimodal and scalable single-cell
1222 analysis. *Nat Biotechnol* **42**, 293-304 (2024).

1223 79. Korsunsky I*, et al.* Fast, sensitive and accurate integration of single-cell data with
1224 Harmony. *Nat Methods* **16**, 1289-1296 (2019).

1225 80. Cremers J, Mulder KT, Klugkist I. Circular interpretation of regression coefficients.
1226 *Br J Math Stat Psychol* **71**, 75-95 (2018).

1227

1228

Figure 1

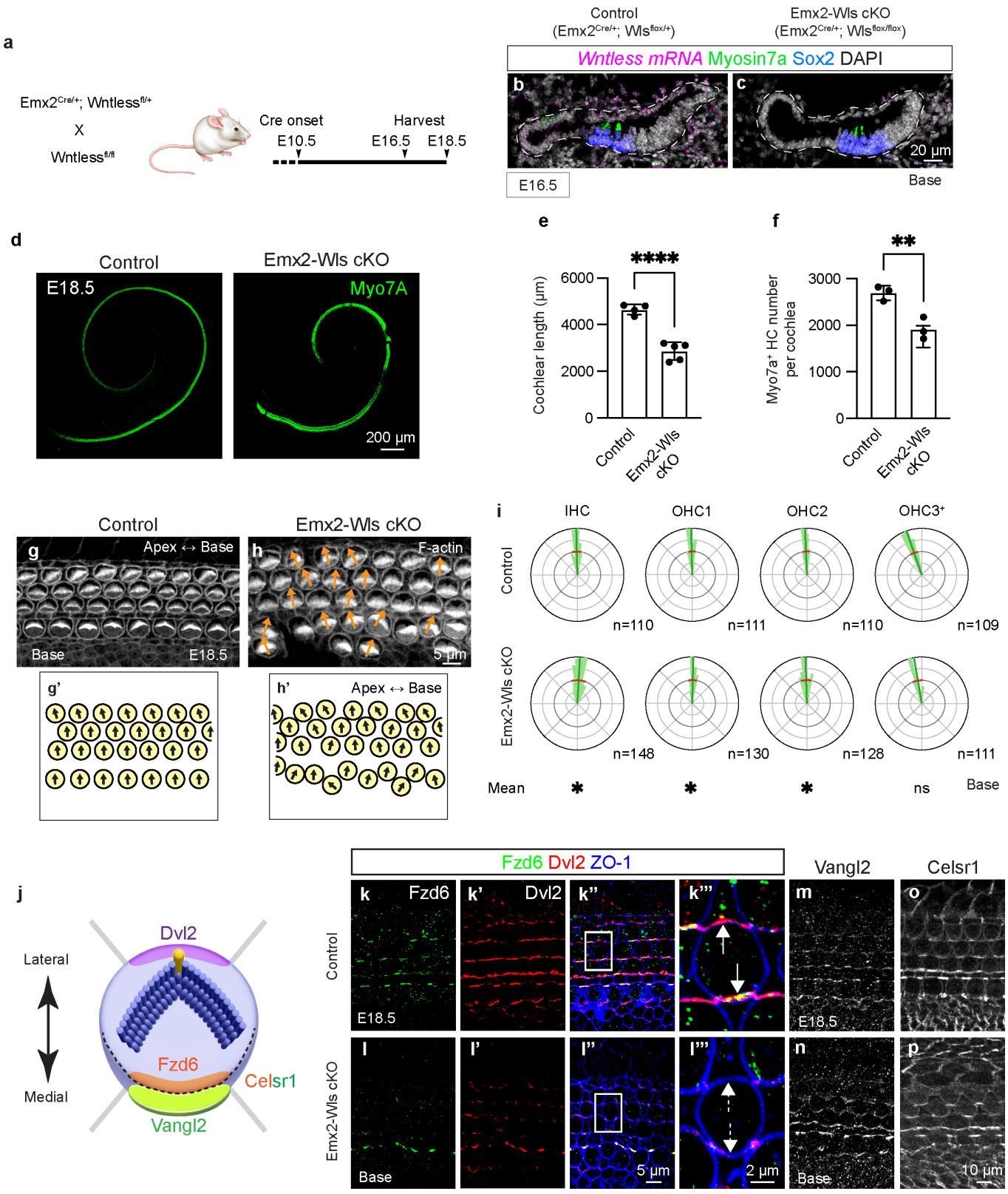
a
Emx2Cre/+; Wntlessfl/+
X
Wntlessfl/fl
Cre onset
E10.5
Harvest
E16.5
E18.5
Control
(Emx2Cre/+; Wlsflox/+)
Emx2-Wls cKO
(Emx2Cre/+; Wlsflox/flox)
Wntless mRNA Myosin7a Sox2 DAPI
b
c
20 µm
E16.5
Base
d
Control
Emx2-Wls cKO
E18.5
Myo7A
200 µm
e
Cochlear length (µm)
6000
4000
2000
0
****
Control
Emx2-Wls cKO
f
Myo7a+ HC number per cochlea
3000
2000
1000
0
**
Control
Emx2-Wls cKO
Control
Emx2-Wls cKO
g
Apex ↔ Base
Base
E18.5
h
F-actin
5 µm
g'
h'
Apex ↔ Base
i
IHC
OHC1
OHC2
OHC3+
Control
Emx2-Wls cKO
n=110
n=111
n=110
n=109
n=148
n=130
n=128
n=111
Mean
*
*
*
ns
Base
j
Lateral
Medial
Dvl2
Fzd6
Celsr1
Vangl2
Fzd6 Dvl2 ZO-1
Vangl2
Celsr1
Control
Emx2-Wls cKO
k
Fzd6
k'
Dvl2
k''
k'''
m
o
E18.5
l
l'
l''
l'''
n
p
Base
5 µm
2 µm
Base
10 µm

Figure 2

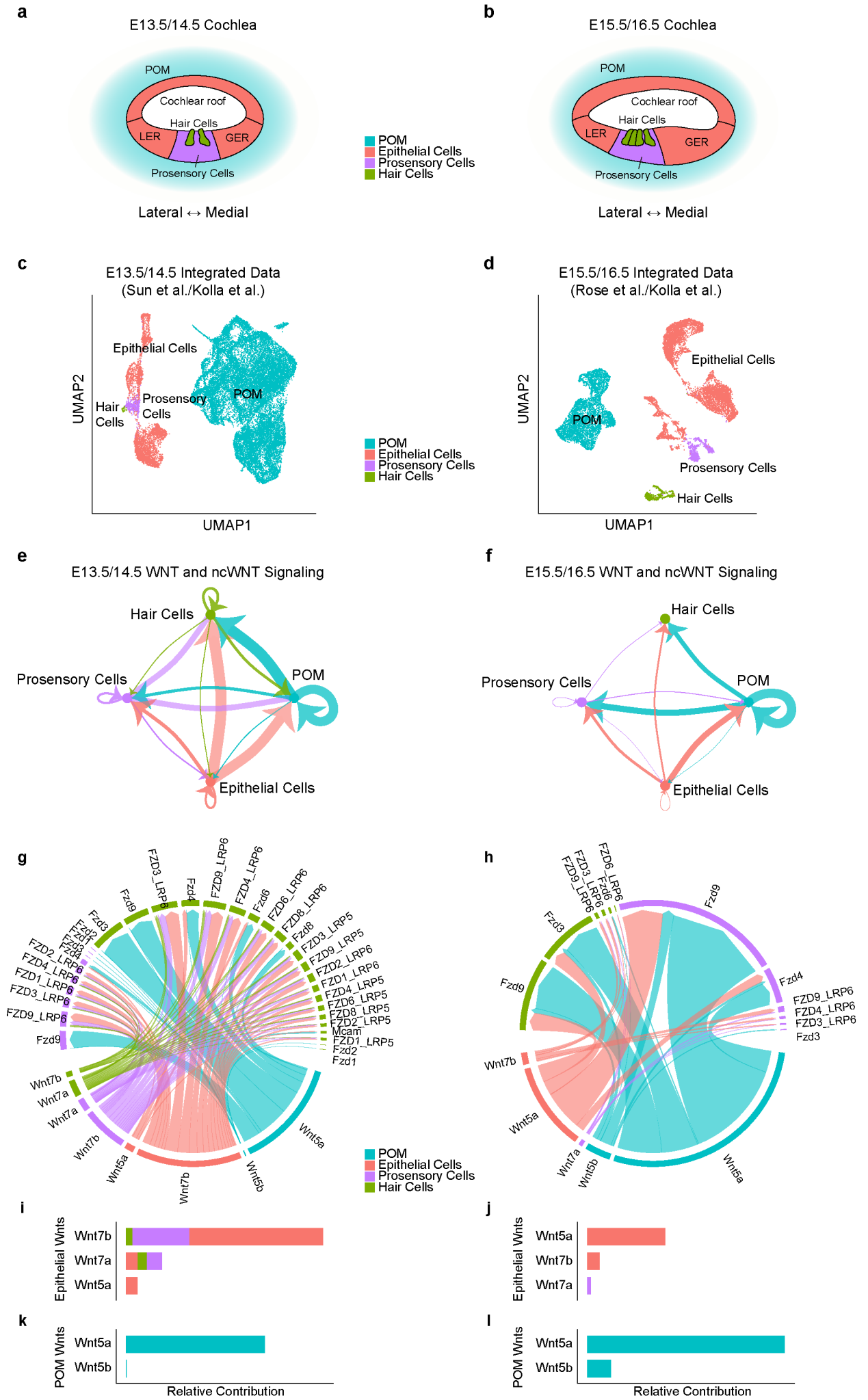
a
E13.5/14.5 Cochlea
POM
Cochlear roof
Hair Cells
LER
GER
Prosensory Cells
Lateral ↔ Medial
POM
Epithelial Cells
Prosensory Cells
Hair Cells
b
E15.5/16.5 Cochlea
POM
Cochlear roof
Hair Cells
LER
GER
Prosensory Cells
Lateral ↔ Medial
c
E13.5/14.5 Integrated Data
(Sun et al./Kolla et al.)
Epithelial Cells
Hair Cells
Prosensory Cells
POM
UMAP2
UMAP1
POM
Epithelial Cells
Prosensory Cells
Hair Cells
d
E15.5/16.5 Integrated Data
(Rose et al./Kolla et al.)
Epithelial Cells
POM
Prosensory Cells
Hair Cells
UMAP2
UMAP1
e
E13.5/14.5 WNT and ncWNT Signaling
Hair Cells
Prosensory Cells
POM
Epithelial Cells
f
E15.5/16.5 WNT and ncWNT Signaling
Hair Cells
Prosensory Cells
POM
Epithelial Cells
g
FZD3_LRP6
FZD9_LRP6
FZD4_LRP6
Fzd4
Fzd6
FZD6_LRP6
FZD8_LRP6
Fzd9
Fzd3
Fzd2
Fzd1
FZD2_LRP6
FZD4_LRP6
FZD1_LRP6
FZD3_LRP6
FZD9_LRP6
Fzd9
FZD3_LRP5
Fzd8
FZD9_LRP5
FZD2_LRP6
FZD1_LRP6
FZD4_LRP5
FZD6_LRP5
FZD8_LRP5
FZD2_LRP5
Mcam
FZD1_LRP5
Fzd2
Fzd1
Wnt7b
Wnt7a
Wnt7a
Wnt7b
Wnt5a
Wnt7b
Wnt5b
Wnt5a
POM
Epithelial Cells
Prosensory Cells
Hair Cells
h
FZD6_LRP6
Fzd6
FZD3_LRP6
FZD9_LRP6
Fzd9
Fzd3
Fzd9
Fzd4
FZD9_LRP6
FZD4_LRP6
FZD3_LRP6
Fzd3
Wnt7b
Wnt5a
Wnt7a
Wnt5b
Wnt5a
i
Epithelial Wnts
Wnt7b
Wnt7a
Wnt5a
j
Epithelial Wnts
Wnt5a
Wnt7b
Wnt7a
k
POM Wnts
Wnt5a
Wnt5b
Relative Contribution
l
POM Wnts
Wnt5a
Wnt5b
Relative Contribution

Figure 3

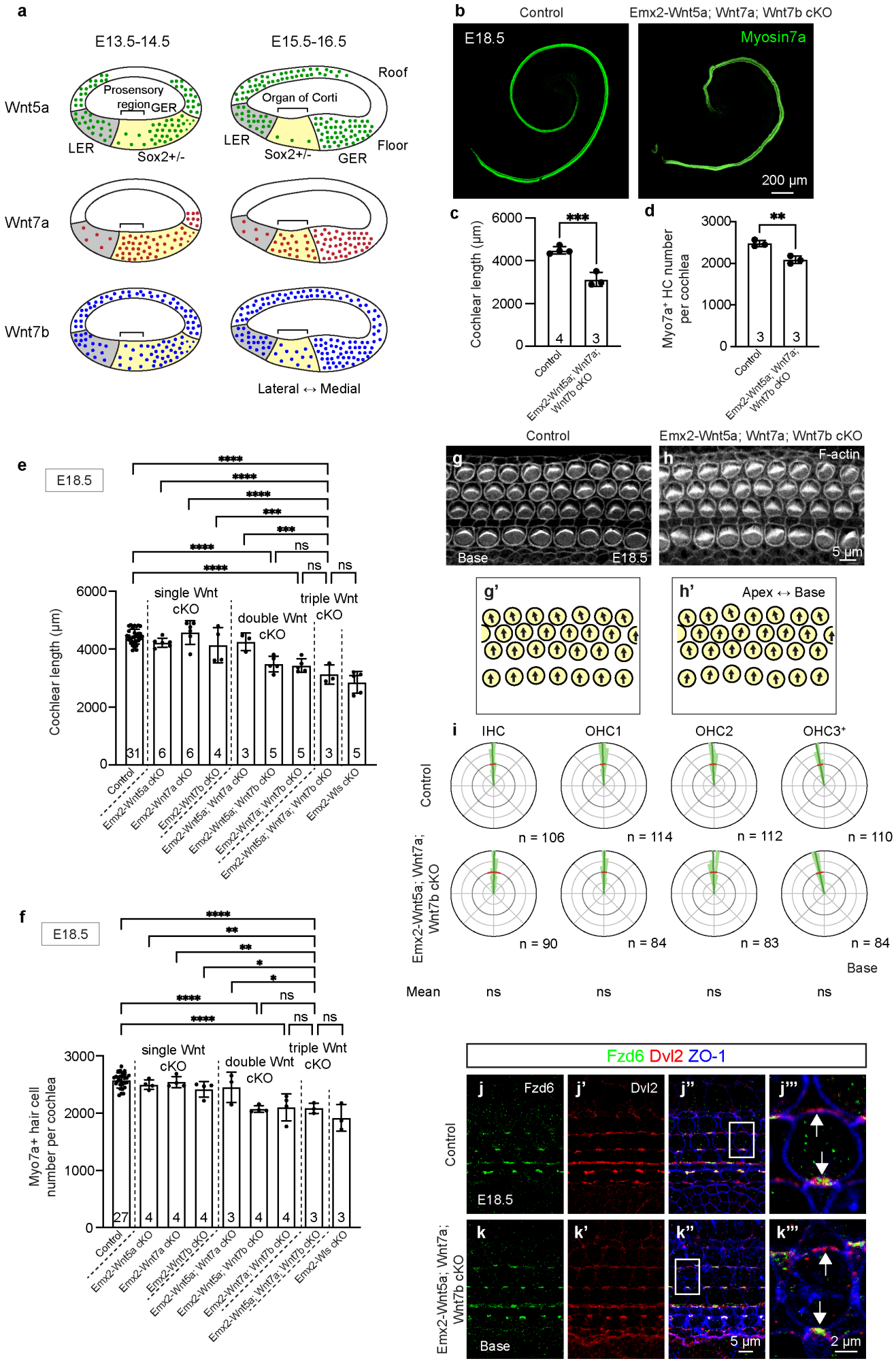
a
E13.5-14.5
E15.5-16.5
Wnt5a
Wnt7a
Wnt7b
Prosensory region
GER
LER
Sox2+/-
Organ of Corti
Roof
Floor
Lateral ↔ Medial
b
Control
Emx2-Wnt5a; Wnt7a; Wnt7b cKO
E18.5
Myosin7a
200 µm
c
Cochlear length (µm)
d
Myo7a+ HC number per cochlea
Control
Emx2-Wnt5a; Wnt7a; Wnt7b cKO
e
E18.5
Cochlear length (µm)
single Wnt cKO
double Wnt cKO
triple Wnt cKO
Control
Emx2-Wnt5a cKO
Emx2-Wnt7a cKO
Emx2-Wnt7b cKO
Emx2-Wnt5a; Wnt7a cKO
Emx2-Wnt5a; Wnt7b cKO
Emx2-Wnt7a; Wnt7b cKO
Emx2-Wnt5a; Wnt7a; Wnt7b cKO
Emx2-Wls cKO
f
E18.5
Myo7a+ hair cell number per cochlea
g
h
F-actin
Base
E18.5
5 µm
g'
h'
Apex ↔ Base
i
IHC
OHC1
OHC2
OHC3+
Control
Emx2-Wnt5a; Wnt7a; Wnt7b cKO
n = 106
n = 114
n = 112
n = 110
n = 90
n = 84
n = 83
n = 84
Base
Mean
ns
Fzd6 Dvl2 ZO-1
j
Fzd6
j'
Dvl2
j''
j'''
k
k'
k''
k'''
E18.5
Base
5 µm
2 µm

Figure 4

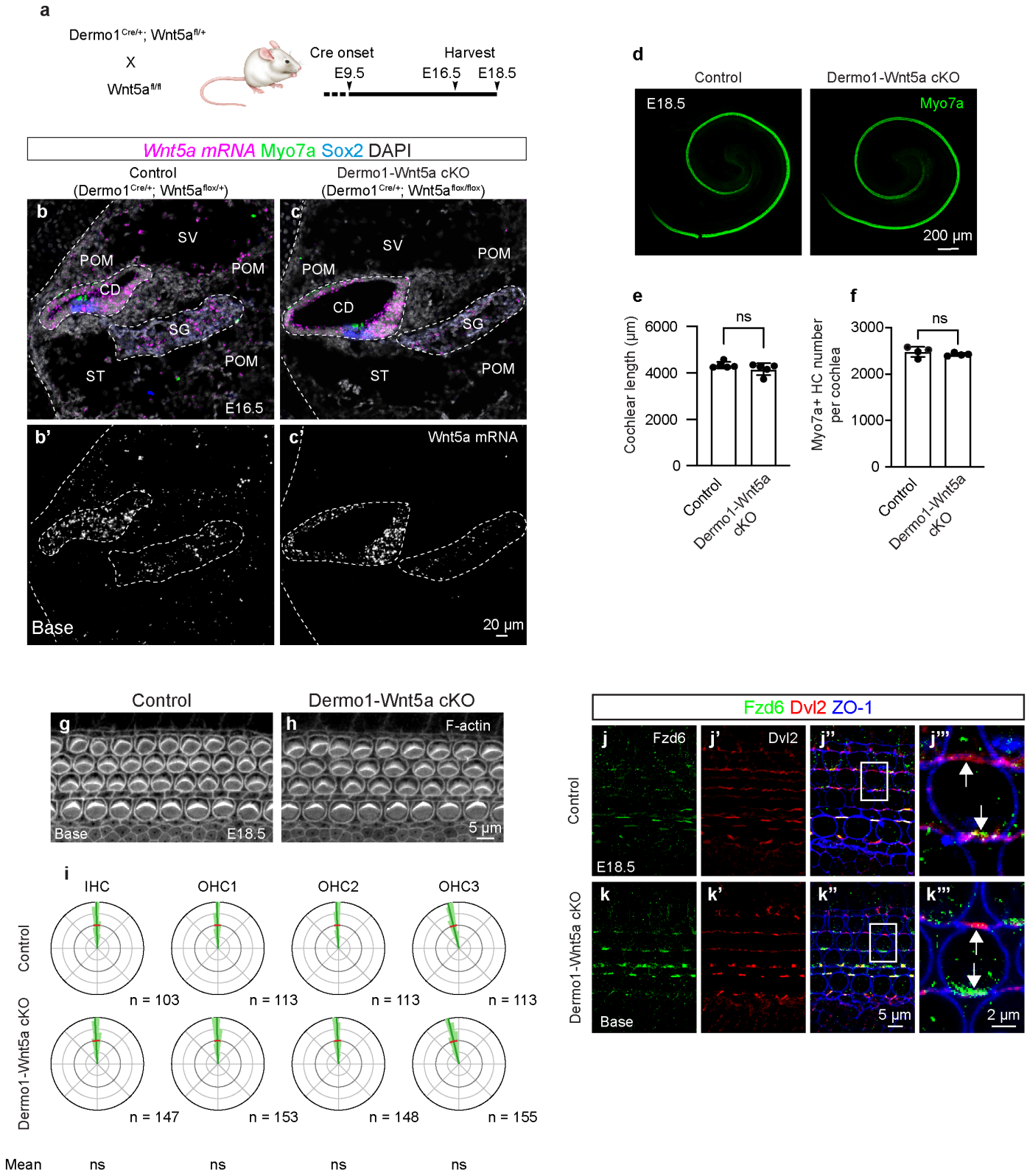
a
Dermo1Cre/+; Wnt5afl/+
X
Wnt5afl/fl
Cre onset
E9.5
Harvest
E16.5
E18.5
Wnt5a mRNA Myo7a Sox2 DAPI
Control
(Dermo1Cre/+; Wnt5aflox/+)
Dermo1-Wnt5a cKO
(Dermo1Cre/+; Wnt5aflox/flox)
b
c
SV
POM
CD
SG
ST
E16.5
b'
c'
Wnt5a mRNA
Base
20 µm
d
Control
Dermo1-Wnt5a cKO
E18.5
Myo7a
200 µm
e
Cochlear length (µm)
6000
4000
2000
0
ns
Control
Dermo1-Wnt5a cKO
f
Myo7a+ HC number per cochlea
3000
2000
1000
0
ns
Control
Dermo1-Wnt5a cKO
Control
Dermo1-Wnt5a cKO
g
h
F-actin
Base
E18.5
5 µm
i
IHC
OHC1
OHC2
OHC3
Control
Dermo1-Wnt5a cKO
n = 103
n = 113
n = 113
n = 113
n = 147
n = 153
n = 148
n = 155
Mean
ns
ns
ns
ns
Fzd6 Dvl2 ZO-1
j
Fzd6
j'
Dvl2
j''
j'''
Control
E18.5
k
k'
k''
k'''
Dermo1-Wnt5a cKO
Base
5 µm
2 µm

Figure 5

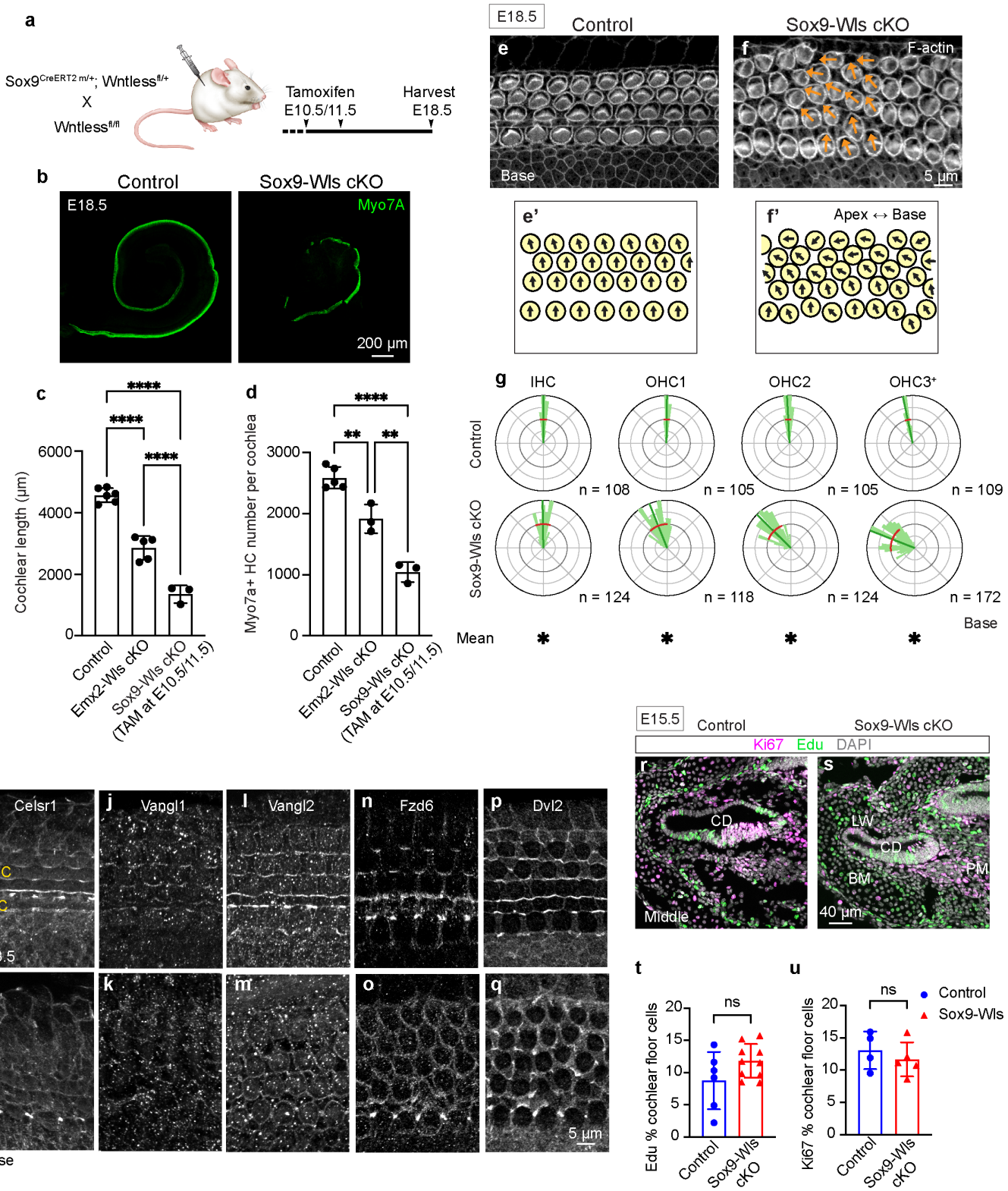
a
Sox9CreERT2 m/+; Wntless fl/+
X
Wntless fl/fl
Tamoxifen
E10.5/11.5
Harvest
E18.5
b
Control
Sox9-Wls cKO
E18.5
Myo7A
200 µm
c
Cochlear length (µm)
Control
Emx2-Wls cKO
Sox9-Wls cKO
(TAM at E10.5/11.5)
d
Myo7a+ HC number per cochlea
e
f
F-actin
Base
5 µm
e'
f'
Apex ↔ Base
g
IHC
OHC1
OHC2
OHC3+
Control
Sox9-Wls cKO
n = 108
n = 105
n = 105
n = 109
n = 124
n = 118
n = 124
n = 172
Base
Mean
h
Celsr1
j
Vangl1
l
Vangl2
n
Fzd6
p
Dvl2
OHC
IHC
E18.5
i
k
m
o
q
5 µm
Base
E15.5
Ki67
Edu
DAPI
r
s
CD
LW
BM
PM
Middle
40 µm
t
Edu % cochlear floor cells
ns
u
Ki67 % cochlear floor cells
Control
Sox9-Wls

Figure 6

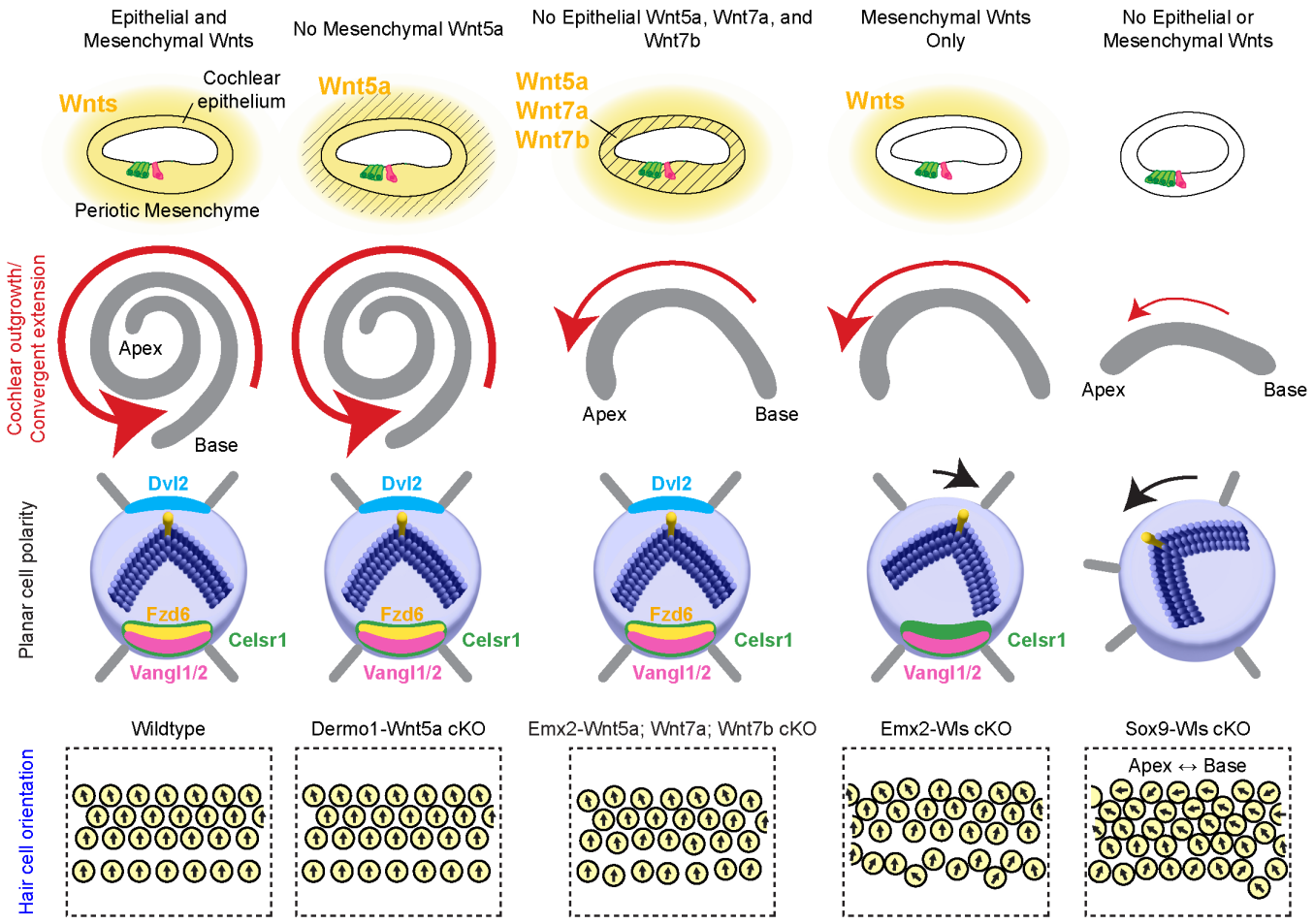
Epithelial and Mesenchymal Wnts
No Mesenchymal Wnt5a
No Epithelial Wnt5a, Wnt7a, and Wnt7b
Mesenchymal Wnts Only
No Epithelial or Mesenchymal Wnts
Wnts
Cochlear epithelium
Periotic Mesenchyme
Wnt5a
Wnt5a
Wnt7a
Wnt7b
Wnts
Cochlear outgrowth/ Convergent extension
Apex
Base
Apex
Base
Apex
Base
Planar cell polarity
Dvl2
Fzd6
Celsr1
Vangl1/2
Hair cell orientation
Wildtype
Dermo1-Wnt5a cKO
Emx2-Wnt5a; Wnt7a; Wnt7b cKO
Emx2-Wls cKO
Sox9-Wls cKO
Apex ↔ Base